

GNSS Receiver Signal Processing Under Spoofing Emile GHIZZO



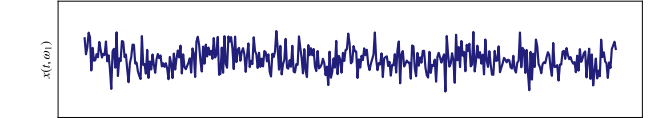
ENAC Telecom, Toulouse

Seminar Presentation

October 17, 2025

A Probabilistic Framework for Non-ergodic Signals

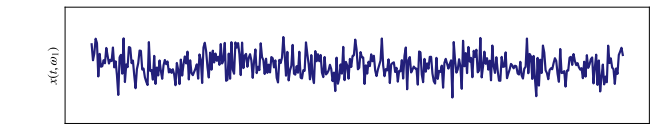
$$y(t,\omega_1) = x(t,\omega_1)$$







$$y(t,\omega_1) = x(t,\omega_1)$$

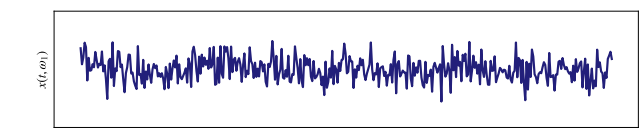




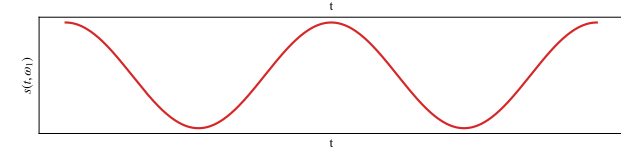




$$y(t,\omega_1) = x(t,\omega_1) + s(t,\omega_1)$$











$$y(t,\omega_1) = x(t,\omega_1) + s(t,\omega_1)$$

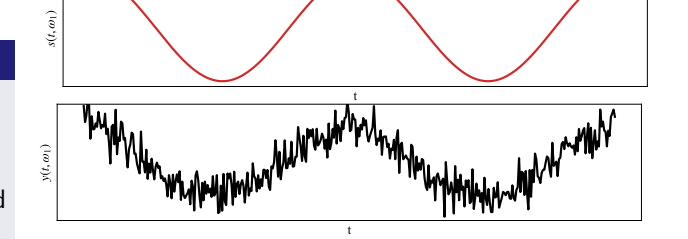




 $p_{x|\{\omega_1\}}(r|\{\omega_1\})$

Ergodicity

Ergodicity allows the statistical properties of a signal to be inferred from a single realization, ω_1 , observed over a time interval I_t .







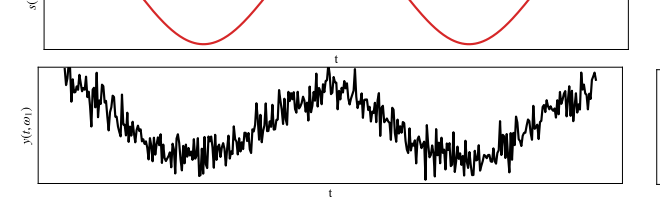
$$y(t,\omega_1) = x(t,\omega_1) + s(t,\omega_1)$$



 $p_{x|\{\omega_1\}}(r|\{\omega_1\})$

Ergodicity

Ergodicity allows the statistical properties of a signal to be inferred from a single realization, ω_1 , observed over a time interval I_t .





 $p_{y|\{\omega_1\}}(r|\{\omega_1\})$

. I RÉPUBLIQUE FRANÇAISE

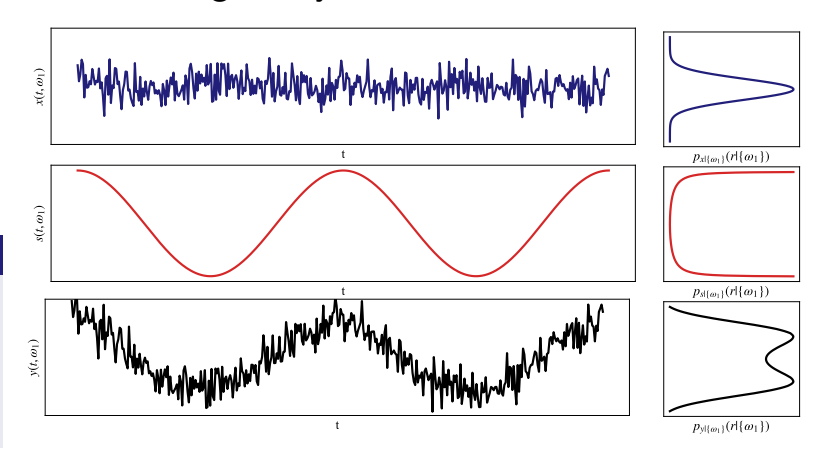


1 / 51

$$y(t,\omega_1) = x(t,\omega_1) + s(t,\omega_1)$$

Ergodicity

Ergodicity allows the statistical properties of a signal to be inferred from a single realization, ω_1 , observed over a time interval I_t .

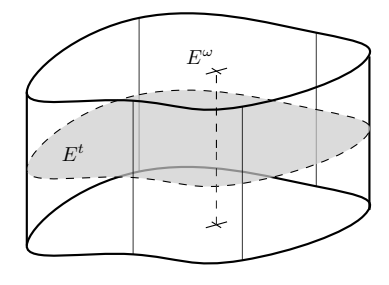


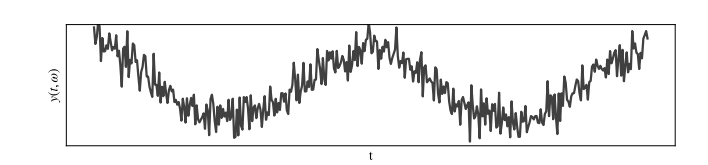




1 / 51

$$(I_t \times I_{\Omega}, \mathcal{E}_{\Omega} \otimes \mathcal{E}_t, \mathbb{P}_{t \times \Omega})$$

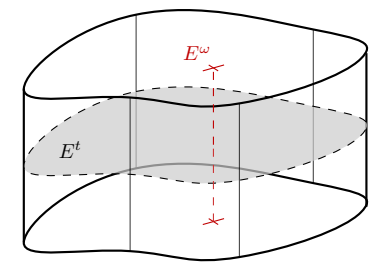








$$(\hspace{.1cm} \emph{l}_{t} \hspace{.1cm} imes \hspace{.1cm} \emph{l}_{\Omega} \hspace{.1cm}, \hspace{.1cm} \mathcal{E}_{\Omega} \hspace{.1cm} \otimes \hspace{.1cm} \mathcal{E}_{t} \hspace{.1cm}, \mathbb{P}_{t \hspace{.1cm} imes \Omega})$$



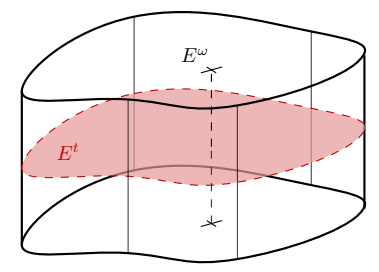
Time probability space:

$$(I_t, \mathcal{E}_t, \mathbb{P}_t)$$



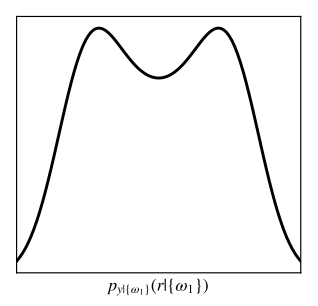


$$(\ \emph{I}_t \ imes \ \emph{I}_\Omega \ , \ \mathcal{E}_\Omega \ \otimes \ \mathcal{E}_t \ , \mathbb{P}_{t imes \ \Omega} \)$$



Random probability space:

$$(I_{\Omega},\mathcal{E}_{\Omega},\mathbb{P}_{\Omega})$$







Measure Theory Framework: Consider the time interval as a probability space, with the observed signal represented as a random variable over the total event space:

- Time Probability Space: Captures the signal realization over time
- Random Probability Space: Captures the randomness of the observed signal.
- Total Probability Space: Combines the time and random realizations of the signal.

Measure Theory Framework





Measure Theory Framework: Consider the time interval as a probability space, with the observed signal represented as a random variable over the total event space:

- Time Probability Space: Captures the signal realization over time
- Random Probability Space: Captures the randomness of the observed signal.
- Total Probability Space: Combines the time and random realizations of the signal.

Measure Theory Framework

✓ Probability theory enables formal definitions of power, distribution, and independence within each probability space.





Measure Theory Framework: Consider the time interval as a probability space, with the observed signal represented as a random variable over the total event space:

- Time Probability Space: Captures the signal realization over time
- Random Probability Space: Captures the randomness of the observed signal.
- Total Probability Space: Combines the time and random realizations of the signal.

Measure Theory Framework

- ✓ Probability theory enables formal definitions of power, distribution, and independence within each probability space.
- ✓ Provides a basis for defining properties such as ergodicity and stationarity.





Measure Theory Framework: Consider the time interval as a probability space, with the observed signal represented as a random variable over the total event space:

- Time Probability Space: Captures the signal realization over time
- Random Probability Space: Captures the randomness of the observed signal.
- Total Probability Space: Combines the time and random realizations of the signal.

Measure Theory Framework

- ✓ Probability theory enables formal definitions of power, distribution, and independence within each probability space.
- ✓ Provides a basis for defining properties such as ergodicity and stationarity.
- ✓ Facilitates the analysis of classical signals (e.g., Markov processes, CW, multiple CWs).





1 / 51

Definition

Context











Definition

Context













Definition

Context















Context Received signal

What is GNSS spoofing?

Definition















What is GNSS spoofing?

Definition

GNSS like signal capable of deceiving a receiver and inducing erroneous Position, Velocity, and Time (PVT) solutions.







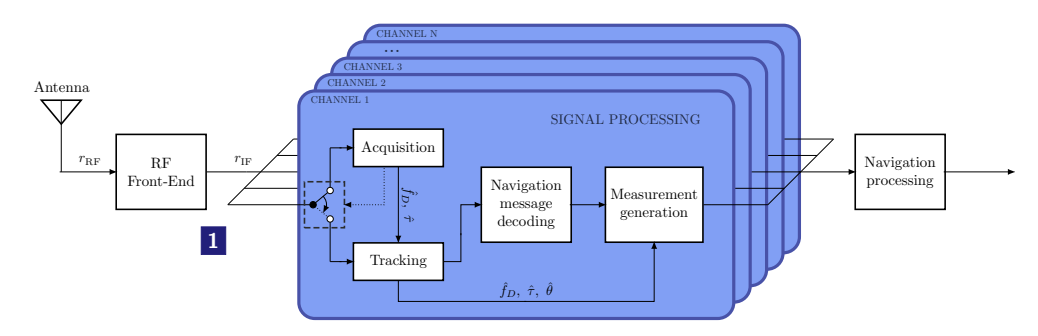


Recorded spoofing events on aircraft receivers (06/11/2025)

https://spoofing.skai-data-services.com/







1

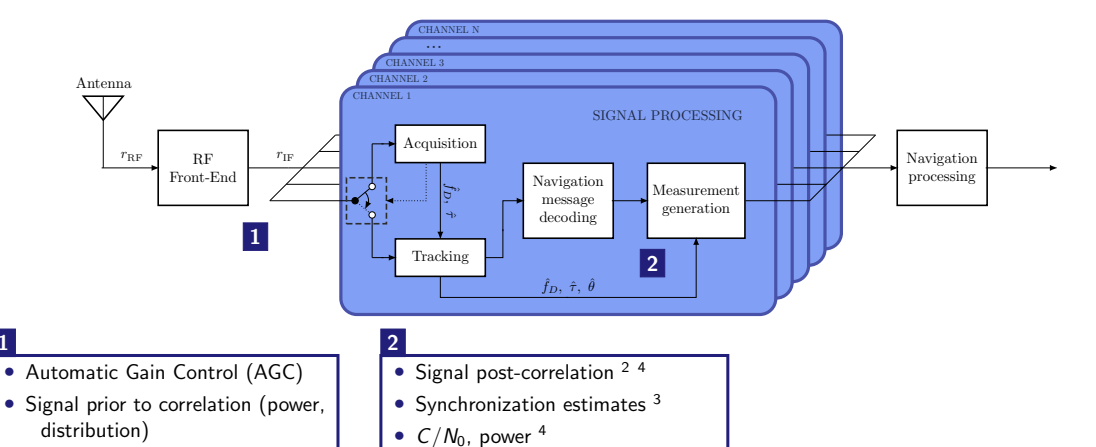
Context

- Automatic Gain Control (AGC) ¹
- • Signal prior to correlation (power, distribution) $^{\mathrm{1}}$





¹ Emile Ghizzo et al. "Assessing jamming and spoofing impacts on GNSS receivers: Automatic gain control (AGC)". In: Signal Processing 228 (2025), p. 109762



³ Emile Ghizzo et al. "Assessing Spoofer Impact on GNSS Receivers: Tracking Loops". In: NAVIGATION: Journal of the Institute of Navigation 72.4 (2025)

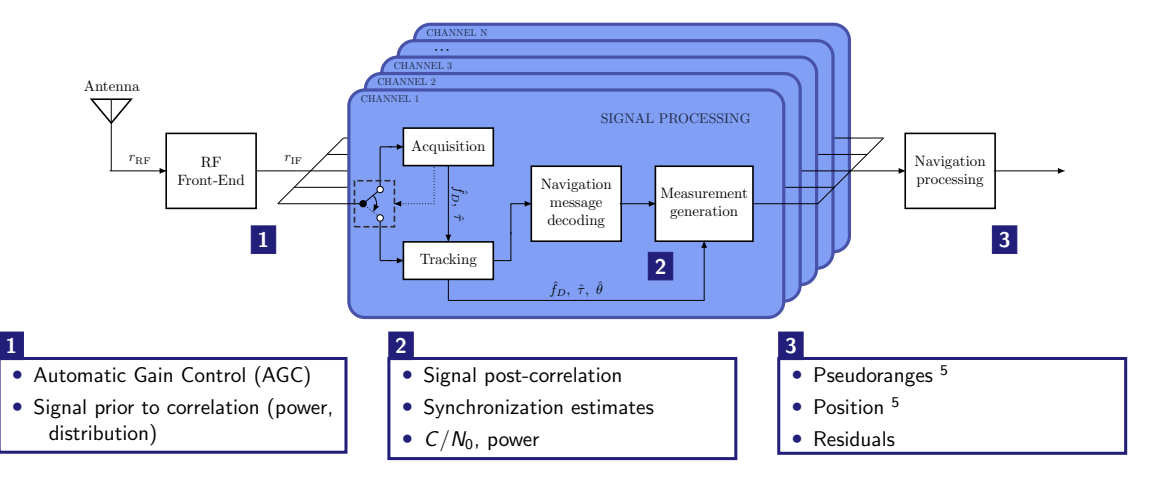






Emile Ghizzo - ENAC

² Mathieu Hussong et al. "Impact of Meaconers on Aircraft GNSS Receivers During Approaches". In: Proc. ION GNSS+ 2023. Sept. 2023, pp. 856-880







3 / 51

⁵ Mathieu Hussong et al. "GNSS performance degradation under meaconing in civil aviation: pseudorange and position models". In: GPS Solutions 29.3 (2025), p. 93

Context 00000

Objectives

Characterize the impact of spoofing on GNSS receiver signal processing, both before and after correlation.







Objectives

Characterize the impact of spoofing on GNSS receiver signal processing, both before and after correlation.

Contributions





Context 00000

Objectives

Characterize the impact of spoofing on GNSS receiver signal processing, both before and after correlation.

Contributions

Introduced a measure-theoretic framework to study time-based estimation under non-ergodic conditions.





4 / 51

Context 00000

Objectives

Characterize the impact of spoofing on GNSS receiver signal processing, both before and after correlation.

Contributions

- Introduced a measure-theoretic framework to study time-based estimation under non-ergodic conditions.
- Derived theoretical models to predict spoofing impact both before correlation and after correlation.





4 / 51



Objectives

Characterize the impact of spoofing on GNSS receiver signal processing, both before and after correlation.

Contributions

- Introduced a measure-theoretic framework to study time-based estimation under non-ergodic conditions.
- Derived theoretical models to predict spoofing impact both before correlation and after correlation.
- Identified specific spoofing situations where GNSS receivers exhibit harmful distortions. including tracking loop chaotic behaviors (e.g., high oscillations, bifurcations) and significant C/N_0 degradation.





Outline

Context

- Context
- 2 Received signal model under spoofing
- 3 Impact of spoofing before correlation
- 4 Impact of spoofing after correlation
- **6** Experimentation
- 6 Conclusion





Outline

Context

- Context
- 2 Received signal model under spoofing
- 3 Impact of spoofing before correlation
- 4 Impact of spoofing after correlation Correlator output Tracking loops C/N_0
- **5** Experimentation
- **6** Conclusion





6 / 51

Outline

Context

00

- 2 Received signal model under spoofing
- 3 Impact of spoofing before correlation
- 4 Impact of spoofing after correlation
- **5** Experimentation





Received signal model

$$\begin{split} r_{\mathsf{RF}}(t) &= \Re \left\{ \left[\sum_{j \in \mathcal{M}_{\mathsf{a}}(t)} \sqrt{C_{\mathsf{a}}^{i}(t)} \; s_{i}(t - \; \tau_{\mathsf{a}}^{i}(t) \;) e^{j \; \theta_{\mathsf{a}}^{i}(t)} \right. \right. \\ &\left. + \sum_{j \in \mathcal{M}_{\mathsf{a}}(t)} \sqrt{C_{\mathsf{s}}^{i}(t) \; s_{j}(t - \; \tau_{\mathsf{s}}^{i}(t) \;) e^{j \; \theta_{\mathsf{a}}^{i}(t)}} \right] \exp \left(2j\pi f_{0} + j\theta_{0}\right) + \; n_{\mathsf{a}}(t) \; + \; n_{\mathsf{s}}(t) \; \right\} \end{split}$$

 $s_i(t)$: GNSS signal of the i^{th} satellite (Navigation message and spreading signal)





Received signal model

$$r_{\mathsf{RF}}(t) = \mathbb{R} \left\{ \left[\sum_{i \in \mathcal{M}_{\mathsf{S}}(t)} \sqrt{C_{\mathsf{a}}^i(t)} \, s_i(t - \tau_{\mathsf{a}}^i(t)) e^{j \, \theta_{\mathsf{a}}^i(t)} \right] + \sum_{i \in \mathcal{M}_{\mathsf{S}}(t)} \sqrt{C_{\mathsf{s}}^i(t)} \, s_i(t - \tau_{\mathsf{s}}^i(t)) e^{j \, \theta_{\mathsf{a}}^i(t)} \right] \exp\left(2j\pi f_0 + j\theta_0\right) + n_{\mathsf{a}}(t) + n_{\mathsf{s}}(t)$$

 $s_i(t)$: GNSS signal of the i^{th} satellite (Navigation message and spreading signal)

 τ_a^i , θ_a^i : Authentic signal code and carrier delay (Doppler modeled by their variation)





Received signal model

$$r_{\mathsf{RF}}(t) = \Re \left\{ \left[\sum_{i \in \mathcal{M}_{\mathsf{a}}(t)} \sqrt{C_{\mathsf{a}}^i(t)} \, s_i(t - \tau_{\mathsf{a}}^i(t)) e^{j \, \theta_{\mathsf{a}}^i(t)} \right] + \sum_{i \in \mathcal{M}_{\mathsf{a}}(t)} \sqrt{C_{\mathsf{s}}^i(t)} \, s_i(t - \tau_{\mathsf{s}}^i(t)) e^{j \, \theta_{\mathsf{a}}^i(t)} \right] \exp \left(2j\pi f_0 + j\theta_0 \right) + \, n_{\mathsf{a}}(t) + \, n_{\mathsf{s}}(t) \, \right\}$$

 $s_i(t)$: GNSS signal of the i^{th} satellite (Navigation message and spreading signal)

 τ_a^i , θ_a^i : Authentic signal code and carrier delay (Doppler modeled by their variation)





$$r_{\mathsf{RF}}(t) = \Re \left\{ \left[\sum_{i \in \mathcal{M}_{\mathsf{a}}(t)} \sqrt{C_{\mathsf{a}}^i(t)} \, s_i(t - \tau_{\mathsf{a}}^i(t)) e^{j \, \theta_{\mathsf{a}}^i(t)} \right] + \sum_{i \in \mathcal{M}_{\mathsf{s}}(t)} \sqrt{C_{\mathsf{s}}^i(t)} \, s_i(t - \tau_{\mathsf{s}}^i(t)) e^{j \, \theta_{\mathsf{a}}^i(t)} \right] \exp \left(2j\pi f_0 + j\theta_0 \right) + n_{\mathsf{a}}(t) + n_{\mathsf{s}}(t)$$

Spoofing dynamic

 $s_i(t)$: GNSS signal of the i^{th} satellite (Navigation message and spreading signal)

 τ_a^i , θ_a^i : Authentic signal code and carrier delay (Doppler modeled by their variation)

 τ_{ϵ}^{i} , θ_{ϵ}^{i} : Spoofing signal code and carrier delay (Doppler modeled by their variation)





$$r_{\mathsf{RF}}(t) = \Re \left\{ \left[\sum_{i \in \mathcal{M}_{\mathsf{a}}(t)} \sqrt{C_{\mathsf{a}}^i(t)} \, s_i(t - au_{\mathsf{a}}^i(t)) e^{j \, heta_{\mathsf{a}}^i(t)} \right] + \sum_{i \in \mathcal{M}_{\mathsf{a}}(t)} \sqrt{C_{\mathsf{s}}^i(t)} \, s_i(t - au_{\mathsf{s}}^i(t)) e^{j \, heta_{\mathsf{a}}^i(t)} \right] \exp \left(2j\pi f_0 + j heta_0 \right) + n_{\mathsf{a}}(t) + n_{\mathsf{s}}(t)$$

 $s_i(t)$: GNSS signal of the i^{th} satellite (Navigation message and spreading signal)

 τ_a^i , θ_a^i : Authentic signal code and carrier delay (Doppler modeled by their variation)

 τ_s^i , θ_s^i : Spoofing signal code and carrier delay (Doppler modeled by their variation)





$$r_{\mathsf{RF}}(t) = \Re \left\{ \left[\sum_{i \in \mathcal{M}_{\mathsf{a}}(t)} \sqrt{C_{\mathsf{a}}^i(t)} \; s_i(t - \tau_{\mathsf{a}}^i(t)) e^{j \; \theta_{\mathsf{a}}^i(t)} \right] + \sum_{i \in \mathcal{M}_{\mathsf{s}}(t)} \sqrt{C_{\mathsf{s}}^i(t)} \; s_i(t - \tau_{\mathsf{s}}^i(t)) e^{j \; \theta_{\mathsf{s}}^i(t)} \right] \exp \left(2j\pi f_0 + j\theta_0 \right) + \; n_{\mathsf{a}}(t) \; + \; n_{\mathsf{s}}(t)$$

 $s_i(t)$: GNSS signal of the i^{th} satellite (Navigation message and spreading signal)

 τ_a^i , θ_a^i : Authentic signal code and carrier delay (Doppler modeled by their variation)

 τ_s^i , θ_s^i : Spoofing signal code and carrier delay (Doppler modeled by their variation)





$$r_{\mathsf{RF}}(t) = \Re \left\{ \left[\sum_{i \in \mathcal{M}_{\mathsf{a}}(t)} \sqrt{C_{\mathsf{a}}^i(t)} \; s_i(t - \tau_{\mathsf{a}}^i(t)) e^{j \; \theta_{\mathsf{a}}^i(t)} \right] + \sum_{i \in \mathcal{M}_{\mathsf{s}}(t)} \sqrt{C_{\mathsf{s}}^i(t)} \; s_i(t - \tau_{\mathsf{s}}^i(t)) e^{j \; \theta_{\mathsf{s}}^i(t)} \right] \exp \left(2j\pi f_0 + j\theta_0 \right) + n_{\mathsf{a}}(t) + n_{\mathsf{s}}(t)$$

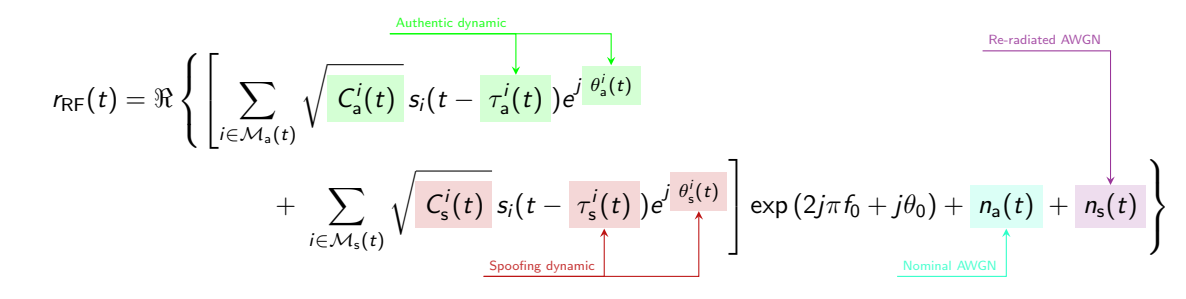
 $s_i(t)$: GNSS signal of the i^{th} satellite (Navigation message and spreading signal)

 τ_a^i , θ_a^i : Authentic signal code and carrier delay (Doppler modeled by their variation)

 τ_{ϵ}^{i} , θ_{ϵ}^{i} : Spoofing signal code and carrier delay (Doppler modeled by their variation)







 $s_i(t)$: GNSS signal of the i^{th} satellite (Navigation message and spreading signal)

 τ_a^i , θ_a^i : Authentic signal code and carrier delay (Doppler modeled by their variation)

 τ_{ϵ}^{i} , θ_{ϵ}^{i} : Spoofing signal code and carrier delay (Doppler modeled by their variation)





Outline

- Context
- 2 Received signal model under spoofing
- 3 Impact of spoofing before correlation
- 4 Impact of spoofing after correlation
- **5** Experimentation
- 6 Conclusion





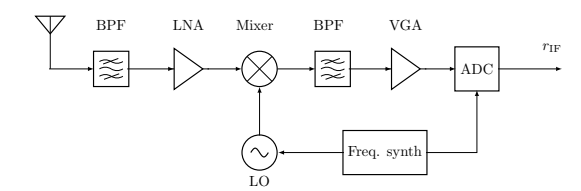
Impact of spoofing on the RFFE

Objectives

- Characterize the signal at RFFE output
- Characterize the AGC dynamic response







Objectives

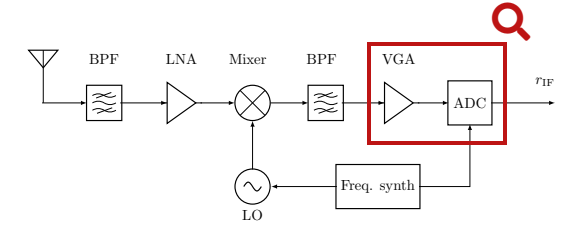
- Characterize the signal at RFFE output
- Characterize the AGC dynamic response





Pre-correlator 000000

Impact of spoofing on the RFFE



Objectives

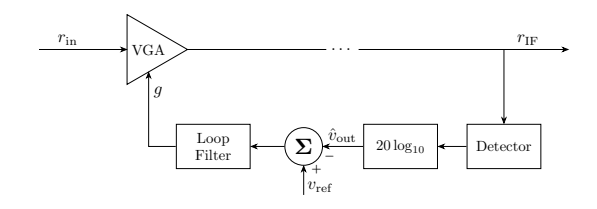
- Characterize the signal at RFFE output
- Characterize the AGC dynamic response





Received signal Pre-correlator Post-correlator Experimentation Conclusion

Impact of spoofing on the RFFE

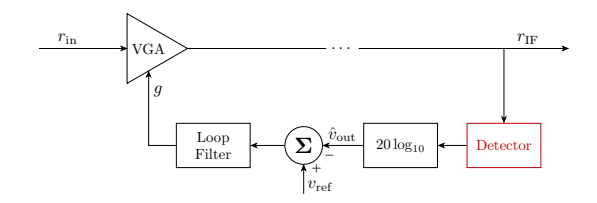


Objectives

- Characterize the signal at RFFE output
- Characterize the AGC dynamic response







Objectives

- Characterize the signal at RFFE output
- Characterize the AGC dynamic response

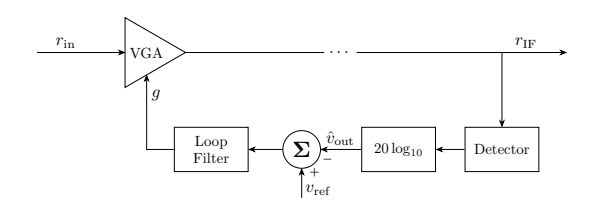
Two Types of Detectors:¹

- Power-based: Computed from the time-domain power over the estimation time I_t.
- **Distribution-based:** Computed from the time-domain distribution over I_t .





¹ Juan Pablo Alegre Pérez, Santiago Celma Pueyo, and Belén Calvo López. Automatic Gain Control. Springer, 2011



AGC dynamic model:

$$g(s) = \frac{F(s)}{1 + F(s)} \left(v_{\text{ref}}(s) - v_{\text{in}}(s) \right)$$
$$v_{\text{out}}(s) = g(s) + v_{\text{in}}(s)$$

Objectives

- Characterize the signal at RFFE output
- Characterize the AGC dynamic response

Two Types of Detectors:¹

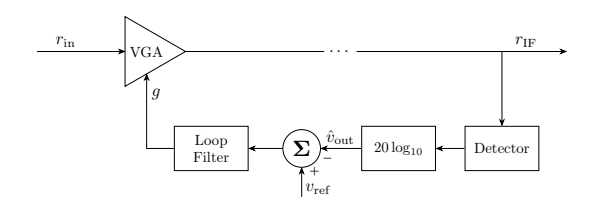
- Power-based: Computed from the time-domain power over the estimation time I_{t} .
- **Distribution-based:** Computed from the time-domain distribution over I_t .





10 / 51

¹ Juan Pablo Alegre Pérez, Santiago Celma Puevo, and Belén Calvo López, Automatic Gain Control. Springer, 2011



AGC dynamic model:

$$g(s) = \frac{F(s)}{1 + F(s)} \left(v_{\text{ref}}(s) - v_{\text{in}}(s) \right)$$

$$\frac{V_{\text{Low-pass filter}}}{V_{\text{out}}(s)} = g(s) + v_{\text{in}}(s)$$

Objectives

- Characterize the signal at RFFE output
- Characterize the AGC dynamic response

Two Types of Detectors:¹

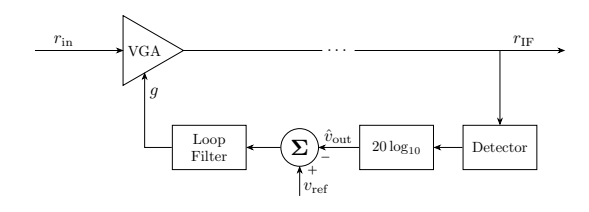
- Power-based: Computed from the time-domain power over the estimation time I_{t} .
- **Distribution-based:** Computed from the time-domain distribution over I_t .





10 / 51

¹ Juan Pablo Alegre Pérez, Santiago Celma Puevo, and Belén Calvo López, Automatic Gain Control. Springer, 2011



AGC dynamic model:

$$g(s) = \frac{F(s)}{1 + F(s)} \left(v_{\text{ref}}(s) - v_{\text{in}}(s) \right)$$

$$\frac{v_{\text{Low-pass filter}}}{v_{\text{out}}(s)} = g(s) + v_{\text{in}}(s)$$

Objectives

- Characterize the signal at RFFE output
- Characterize the AGC dynamic response

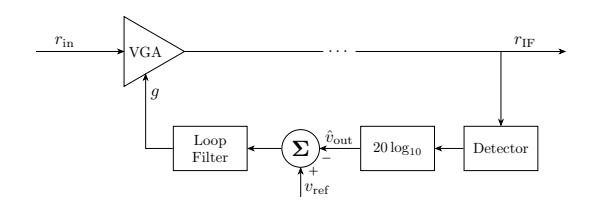
Two Types of Detectors:¹

- Power-based: Computed from the time-domain power over the estimation time I_t.
- **Distribution-based:** Computed from the time-domain distribution over I_t .

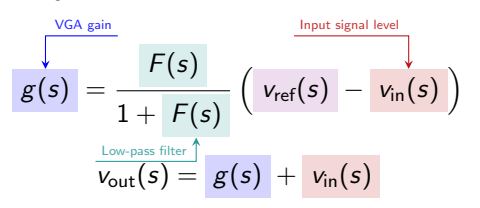




¹ Juan Pablo Alegre Pérez, Santiago Celma Pueyo, and Belén Calvo López. Automatic Gain Control. Springer, 2011



AGC dynamic model:



Objectives

- Characterize the signal at RFFE output
- Characterize the AGC dynamic response

Two Types of Detectors:¹

- Power-based: Computed from the time-domain power over the estimation time I_{t} .
- **Distribution-based:** Computed from the time-domain distribution over I_t .





10 / 51

¹ Juan Pablo Alegre Pérez, Santiago Celma Puevo, and Belén Calvo López, Automatic Gain Control. Springer, 2011

Spoofing impact on signal level

Signal Level v

Describes the strength of the signal r. It can be defined through the signal power or its distribution within the estimation interval I_t , depending on the type of detector.





Spoofing impact on signal level

Signal Level v

Describes the strength of the signal r. It can be defined through the signal power or its distribution within the estimation interval I_t , depending on the type of detector.

$$r_{\mathsf{s}}(t) = \sum_{m=1}^{M} a_{\mathsf{s},m} s_{m} \left(t - \tau_{\mathsf{s},m}\right) \cos\left(2\pi f_{m} t + \theta_{m}\right)$$





Spoofing impact on signal level

Signal Level v

Describes the strength of the signal r. It can be defined through the signal power or its distribution within the estimation interval I_t , depending on the type of detector.

$$r_{
m s}(t) = \sum_{m=1}^{M} egin{array}{c} s_{
m in} & s_{
m in} & \left(t - au_{
m s,m}
ight) \cos\left(2\pi au_{
m in} t + heta_{
m in}
ight) \end{array}$$





Spoofing impact on signal level

Signal Level v

Describes the strength of the signal r. It can be defined through the signal power or its distribution within the estimation interval I_t , depending on the type of detector.

$$r_{\rm S}(t) = \sum_{m=1}^{M} \frac{a_{\rm S,m} \ s_m}{a_{\rm S,m} \ s_m} \left(t - \frac{\tau_{\rm S,m}}{\tau_{\rm S,m}}\right) \cos\left(2\pi \frac{f_m}{t} t + \frac{\theta_m}{t}\right)$$

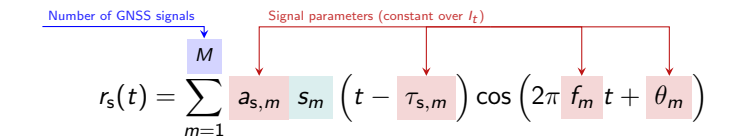




Spoofing impact on signal level

Signal Level v

Describes the strength of the signal r. It can be defined through the signal power or its distribution within the estimation interval I_t , depending on the type of detector.





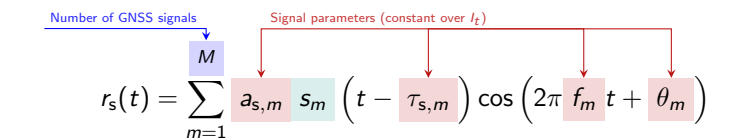


Spoofing impact on signal level

Signal Level v

Describes the strength of the signal r. It can be defined through the signal power or its distribution within the estimation interval I_t , depending on the type of detector.

Spoofing signal model:



Results

The input signal level v_{in} (and, consequently, the AGC) can be determined by computing its power and distribution.



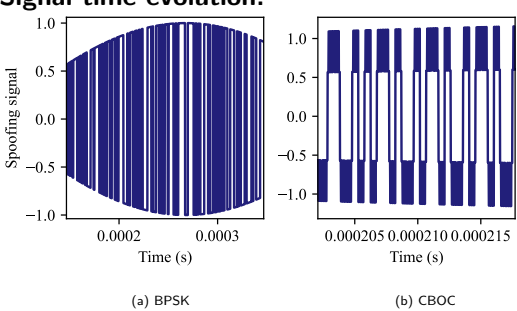


Individual PRN spoofing signal (M = 1)

Results

The individual PRN signal is shown to be equivalent to a weighted **continuous wave (CW)**, modeled through the proposed **measure theory framework**.

Signal time evolution:





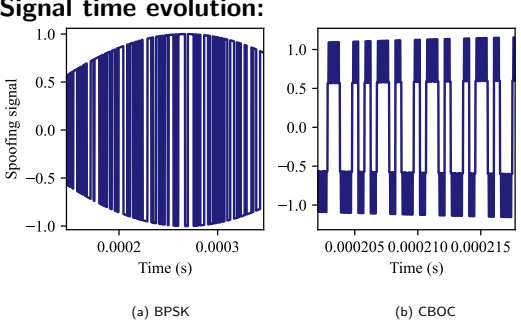


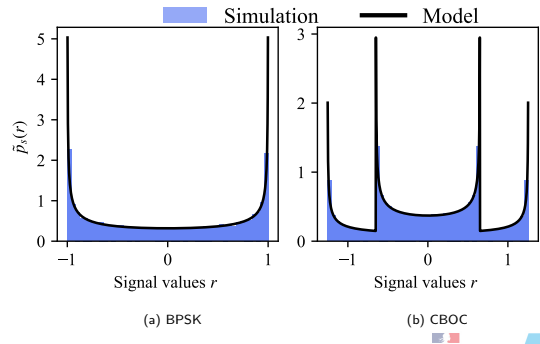
Individual PRN spoofing signal (M = 1)

Results

The individual PRN signal is shown to be equivalent to a weighted continuous wave (CW), modeled through the proposed measure theory framework.

Signal time evolution:





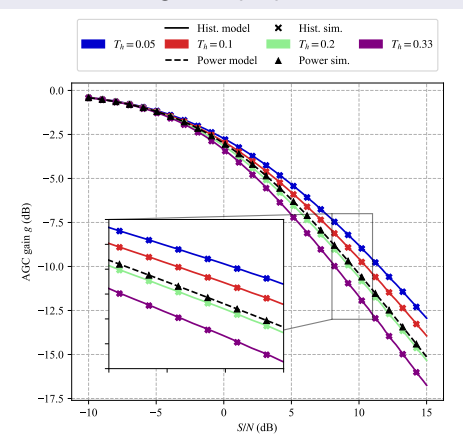


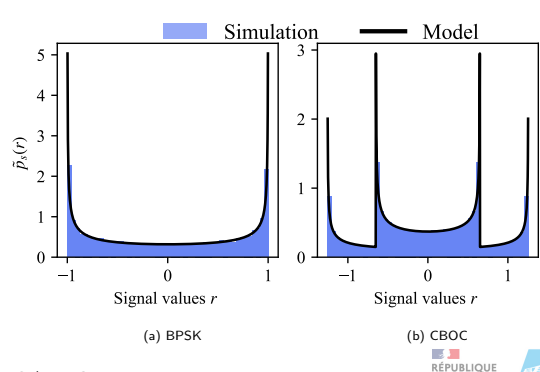


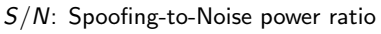
Individual PRN spoofing signal (M = 1)

Results

The individual PRN signal is shown to be equivalent to a weighted **continuous wave (CW)**, modeled through the proposed **measure theory framework**.









FRANÇAISE

Multiple PRN Spoofing Signal (M > 1)

Signal distribution (M=2):

Simulation

Model

Results

• Equivalent to multiple weighted CWs.

(a) BPSK

(b) CBOC





Pre-correlator 000000

Multiple PRN Spoofing Signal (M > 1)

Signal distribution (M=2):

Simulation

Model 1

Results

- Equivalent to multiple weighted CWs.
- Distribution depends on the relative amplitudes between CWs.

(a) BPSK

(b) CBOC

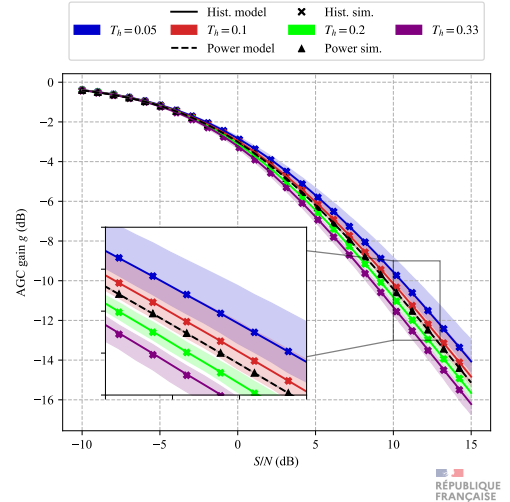




Multiple PRN Spoofing Signal (M > 1)

Results

- Equivalent to multiple weighted CWs.
- Distribution depends on the relative amplitudes between CWs.





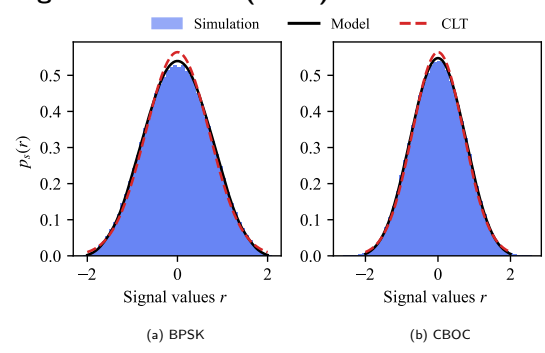


Multiple PRN Spoofing Signal (M > 1)

Results

- Equivalent to multiple weighted CWs.
- Distribution depends on the relative amplitudes between CWs.
- The signal converges toward a normal distribution as $M \to +\infty$ (Central Limit Theorem, CLT).

Signal distribution (M=5):







Conclusion on spoofing impact before correlation

Spoofing Impact Before Correlation

The AGC dynamic response can be characterized through the input signal level (and thus signal power and distribution).

The spoofing impact can be modeled as weighted continuous waves (CWs), analyzed similarly to a jammer:

- M=1: Equivalent to a single weighted CW.
- M > 1: Equivalent to multiple weighted CWs.
- $M \to \infty$: Converges toward a normal distribution.

Spoofing acts as a multiple weighted CW jammer for the AGC, starting to impact **AGC** values for S/N > -5 dB.





14 / 51

¹Emile Ghizzo et al. "Assessing iamming and spoofing impacts on GNSS receivers: Automatic gain control (AGC)", In: Signal Processing 228 (2025), p. 109762

ceived signal Pre-correlator Post-corre

Outline

- Context
- 2 Received signal model under spoofing
- 3 Impact of spoofing before correlation
- 4 Impact of spoofing after correlation Correlator output Tracking loops C/N_0
- **5** Experimentation
- 6 Conclusion





Outline

- Context
- 2 Received signal model under spoofing
- 3 Impact of spoofing before correlation
- 4 Impact of spoofing after correlation Correlator output

Tracking loops C/N_0

- **5** Experimentation
- 6 Conclusion





$$\Lambda(\boldsymbol{\eta}) = \frac{1}{T_{\mathsf{i}}} \int_{t_{\mathsf{i}}}^{(k+1)} f_{\mathsf{i}}(t) c^{*}(t-\tau) \exp\left(-2j\pi t(f_{\mathsf{i}\mathsf{F}}+f) - j(\theta-\pi T_{\mathsf{i}}f)\right) dt, \quad \forall \boldsymbol{\eta} = [\tau,\theta,f]^{\mathsf{T}}$$





$$\Lambda(\boldsymbol{\eta}) = \frac{1}{T_{i}} \int_{t_{i}}^{(k+1)} \int_{t_{i}}^{T_{i}} \eta_{\mathsf{F}}(t) \ c^{*}(t-\boldsymbol{\tau}) \exp\left(-2j\pi t(f_{\mathsf{IF}}+\boldsymbol{f}) - j(\boldsymbol{\theta}-\pi T_{i}|\boldsymbol{f})\right) \mathrm{d}t, \quad \forall \boldsymbol{\eta} = [\tau, \theta, f]^{\mathsf{T}}$$





$$\Lambda(\begin{array}{c} \boldsymbol{\eta} \end{array}) = \frac{1}{T_{\mathrm{i}}} \int\limits_{kT_{\mathrm{i}}}^{(k+1)T_{\mathrm{i}}} \eta_{\mathrm{F}}(t) \ c^{*}(t-\tau) \exp\left(-2j\pi t (f_{\mathrm{iF}} + f) - j(\begin{array}{c} \theta \end{array} - \pi T_{\mathrm{i}} f \end{array})\right) \mathrm{d}t, \quad \forall \boldsymbol{\eta} = [\tau, \theta, f]^{\mathsf{T}}$$
Integration time \uparrow





$$\Lambda(\begin{array}{c} \boldsymbol{\eta} \end{array}) = \frac{1}{T_{\mathrm{i}}} \int\limits_{kT_{\mathrm{i}}}^{(k+1)} \int\limits_{kT_{\mathrm{i}}}^{r_{\mathrm{i}}} r_{\mathrm{i}}(t) c^{*}(t-\tau) \exp\left(-2j\pi t(f_{\mathrm{i}} + |f|) - j(|\theta| - \pi T_{\mathrm{i}}|f|)\right) \mathrm{d}t, \quad \forall \boldsymbol{\eta} = [\tau, \theta, f]^{\mathsf{T}}$$
Integration time \(\begin{align*} \text{Neceived signal} \)





$$\Lambda(\begin{array}{c} \boldsymbol{\eta} \end{array}) = \frac{1}{T_{\mathrm{i}}} \int\limits_{k T_{\mathrm{i}}}^{(k+1) T_{\mathrm{i}}} r_{\mathrm{IF}}(t) c^{*}(t-\tau) \exp\left(-2j\pi t(f_{\mathrm{IF}} + |f|) - j(|\theta| - \pi T_{\mathrm{i}}|f|)\right) \mathrm{d}t, \quad \forall \boldsymbol{\eta} = [\tau, \theta, f]^{\mathsf{T}}$$

$$\uparrow \text{Received signal}$$

$$n_{\mathsf{F}}(t) = \left[\sum_{i \in \mathcal{M}_{\mathsf{a}}} r_{\mathsf{a}}^i(t, \boldsymbol{\eta}_{\mathsf{a}}^i) + \sum_{i \in \mathcal{M}_{\mathsf{s}}} r_{\mathsf{s}}^i(t, \boldsymbol{\eta}_{\mathsf{s}}^i) \right] \exp\left(2j\pi f_{\mathsf{IF}} + j\theta_{\mathsf{IF}}\right) + n_{\mathsf{a}}(t) + n_{\mathsf{s}}(t)$$





$$\Lambda(\begin{array}{c} \boldsymbol{\eta} \end{array}) = \frac{1}{T_{\mathrm{i}}} \int\limits_{kT_{\mathrm{i}}}^{(k+1)T_{\mathrm{i}}} \eta_{\mathrm{F}}(t) \ c^{*}(t-\tau) \exp\left(-2j\pi t(f_{\mathrm{IF}}+f) - j(\begin{array}{c} \theta \end{array} - \pi T_{\mathrm{i}} f \end{array})\right) \mathrm{d}t, \quad \forall \boldsymbol{\eta} = [\tau, \theta, f]^{\mathsf{T}}$$
Integration time

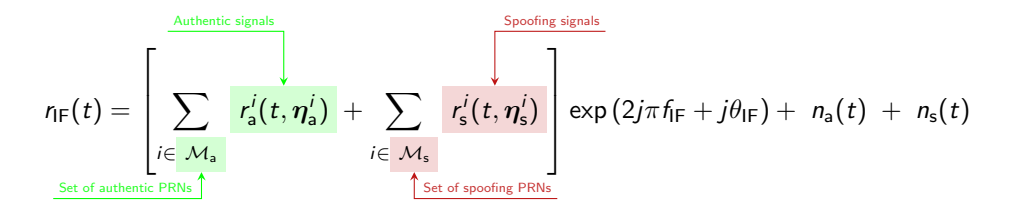
Post-correlator

$$r_{\mathsf{IF}}(t) = \left[\sum_{\substack{i \in \mathcal{M}_{\mathsf{a}} \\ \mathsf{Set of authentic PRNs} \uparrow}}^{\substack{\mathsf{Authentic signals} \\ r_{\mathsf{a}}^i(t, \eta_{\mathsf{a}}^i)} + \sum_{\substack{i \in \mathcal{M}_{\mathsf{s}} \\ i \in \mathcal{M}_{\mathsf{s}}}} r_{\mathsf{s}}^i(t, \eta_{\mathsf{s}}^i) \right] \exp\left(2j\pi f_{\mathsf{IF}} + j\theta_{\mathsf{IF}}\right) + n_{\mathsf{a}}(t) + n_{\mathsf{s}}(t)$$





$$\Lambda(\begin{array}{c} \boldsymbol{\eta} \end{array}) = \frac{1}{T_{\mathrm{i}}} \int\limits_{k T_{\mathrm{i}}}^{(k+1) T_{\mathrm{i}}} \eta_{\mathrm{F}}(t) c^{*}(t-\tau) \exp\left(-2j\pi t(f_{\mathrm{iF}} + f) - j(\begin{array}{c} \theta \end{array} - \pi T_{\mathrm{i}} f \end{array})\right) \mathrm{d}t, \quad \forall \boldsymbol{\eta} = [\tau, \theta, f]^{\mathsf{T}}$$
Integration time

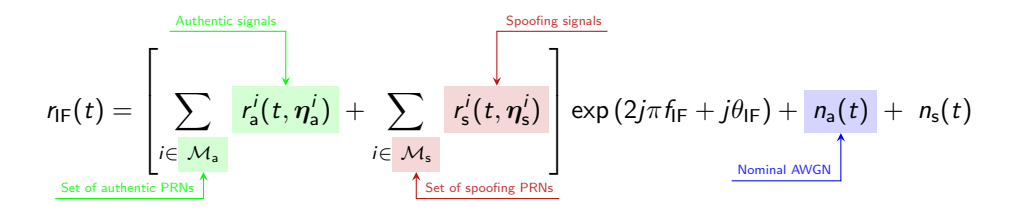






$$\Lambda(\begin{array}{c} \boldsymbol{\eta} \end{array}) = \frac{1}{T_{\mathrm{i}}} \int\limits_{k T_{\mathrm{i}}}^{(k+1)} \int\limits_{k T_{\mathrm{i}}}^{r_{\mathrm{i}}} r_{\mathrm{i}}(t) c^{*}(t-\tau) \exp\left(-2j\pi t(f_{\mathrm{iF}} + f) - j(\theta - \pi T_{\mathrm{i}} f)\right) \mathrm{d}t, \quad \forall \boldsymbol{\eta} = [\tau, \theta, f]^{\mathsf{T}}$$

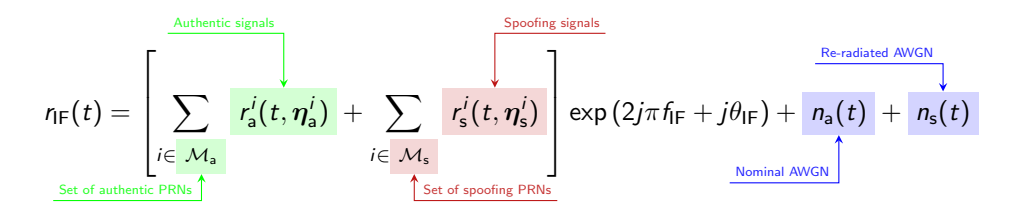
$$\uparrow_{\mathrm{Integration time}} \uparrow_{\mathrm{Received signal}}$$







$$\Lambda(\begin{array}{c} \boldsymbol{\eta} \end{array}) = \frac{1}{T_{\mathrm{i}}} \int\limits_{kT_{\mathrm{i}}}^{(k+1)} \int\limits_{kT_{\mathrm{i}}}^{r_{\mathrm{i}}} r_{\mathrm{i}}(t) c^{*}(t-\tau) \exp\left(-2j\pi t(f_{\mathrm{iF}}+|f|) - j(|\theta|-\pi T_{\mathrm{i}}|f|)\right) \mathrm{d}t, \quad \forall \boldsymbol{\eta} = [\tau,\theta,f]^{\mathsf{T}}$$
Integration time \(\frac{1}{2}\) \(\text{Received signal}\)

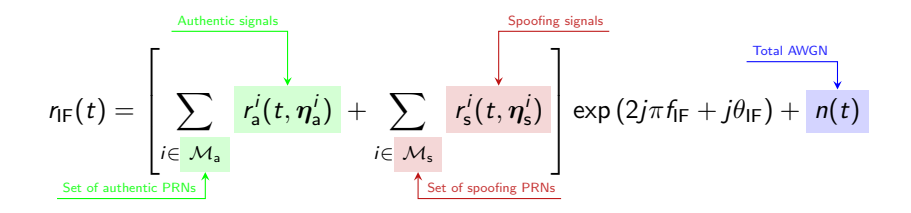






$$\Lambda(\begin{array}{c} \boldsymbol{\eta} \end{array}) = \frac{1}{T_{\mathrm{i}}} \int\limits_{k T_{\mathrm{i}}}^{(k+1) T_{\mathrm{i}}} \eta_{\mathrm{F}}(t) \ c^{*}(t-\tau) \exp\left(-2j\pi t(f_{\mathrm{iF}} + f) - j(\begin{array}{c} \theta \end{array} - \pi T_{\mathrm{i}} f \end{array})\right) \mathrm{d}t, \quad \forall \boldsymbol{\eta} = [\tau, \theta, f]^{\mathsf{T}}$$

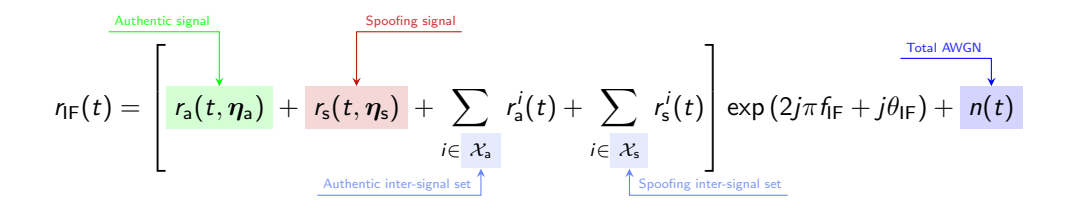
$$\uparrow_{\mathrm{Integration time}} \uparrow_{\mathrm{Integration time}} \uparrow_{\mathrm{Received signal}}$$







$$\Lambda(\begin{array}{c} \boldsymbol{\eta} \end{array}) = \frac{1}{T_{\mathrm{i}}} \int\limits_{kT_{\mathrm{i}}}^{(k+1)} \int\limits_{kT_{\mathrm{i}}}^{r_{\mathrm{i}}} r_{\mathrm{i}}(t) c^{*}(t-\tau) \exp\left(-2j\pi t(f_{\mathrm{iF}}+|f|) - j(|\theta|-\pi T_{\mathrm{i}}|f|)\right) \mathrm{d}t, \quad \forall \boldsymbol{\eta} = [\tau,\theta,f]^{\mathsf{T}}$$
Integration time \(\frac{1}{2}\) \(\text{Received signal}\)







$$r_{\rm IF}(t) = \begin{bmatrix} r_{\rm a}(t,\eta_{\rm a}) + r_{\rm s}(t,\eta_{\rm s}) \\ \end{bmatrix} + \chi(t) \exp(2j\pi f_{\rm IF} + j\theta_{\rm IF}) + \eta(t)$$

 $\chi(t)$ is shown as a **Gaussian random variable** (CLT)





$$\Lambda(\boldsymbol{\eta}, \boldsymbol{\eta}_{\mathsf{a}}, \boldsymbol{\eta}_{\mathsf{s}}) = \Lambda_{\mathsf{a}}(\boldsymbol{\eta}_{\mathsf{a}} - \boldsymbol{\eta}) + \Lambda_{\mathsf{s}}(\boldsymbol{\eta}_{\mathsf{s}} - \boldsymbol{\eta}) + \Lambda_{\chi} + \Lambda_{n}$$





$$\Lambda(\eta, \eta_{\mathsf{a}}, \eta_{\mathsf{s}}) = \Lambda_{\mathsf{a}}(\eta_{\mathsf{a}} - \eta) + \Lambda_{\mathsf{s}}(\eta_{\mathsf{s}} - \eta) + \Lambda_{\chi} + \Lambda_{\eta}$$

• Authentic peak:

$$\Lambda_{\rm a}(\eta_{\rm a}\!-\!\eta) = \sqrt{C_{\rm a}}\,d_k\,\zeta_\tau(\tau_{\rm a}\!-\!\tau)\,\zeta_f(f_{\rm a}\!-\!f)\,e^{j(\theta_{\rm a}-\theta)}$$





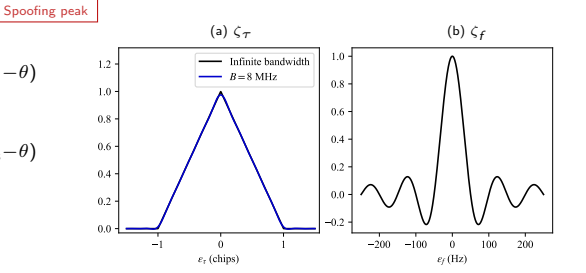
$$\Lambda(\eta, \eta_{\mathsf{a}}, \eta_{\mathsf{s}}) = \Lambda_{\mathsf{a}}(\eta_{\mathsf{a}} - \eta) + \Lambda_{\mathsf{s}}(\eta_{\mathsf{s}} - \eta) + \Lambda_{\chi} + \Lambda_{\eta}$$

Authentic peak:

$$\Lambda_{a}(\eta_{a}-\eta) = \sqrt{C_{a}} d_{k} \zeta_{\tau}(\tau_{a}-\tau) \zeta_{f}(f_{a}-f) e^{j(\theta_{a}-\theta)}$$

Spoofing peak:

$$\Lambda_{s}(\boldsymbol{\eta}_{s}-\boldsymbol{\eta}) = \sqrt{C_{s}} d_{k} \zeta_{\tau}(\tau_{s}-\tau) \zeta_{f}(f_{s}-f) e^{j(\theta_{s}-\theta)}$$







18 / 51

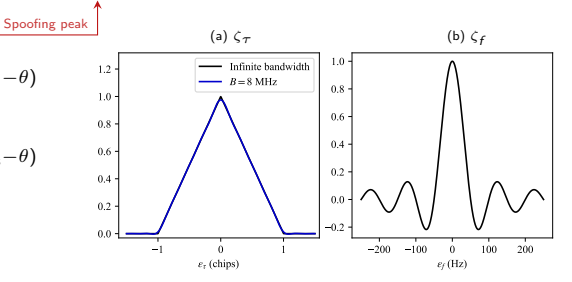
$$\Lambda(\eta, \eta_{\mathsf{a}}, \eta_{\mathsf{s}}) = \Lambda_{\mathsf{a}}(\eta_{\mathsf{a}} - \eta) + \Lambda_{\mathsf{s}}(\eta_{\mathsf{s}} - \eta) + \Lambda_{\chi} + \Lambda_{\eta}$$

Authentic peak:

$$\Lambda_{\rm a}(\eta_{\rm a}\!-\!\eta) = \sqrt{C_{\rm a}}\,d_k\,\zeta_{ au}(au_{
m a}\!-\! au)\,\zeta_f(f_{
m a}\!-\!f)\,{
m e}^{j(heta_{
m a}- heta)}$$

Spoofing peak:

$$\Lambda_{s}(\eta_{s}-\eta) = \sqrt{C_{s}} d_{k} \zeta_{\tau}(\tau_{s}-\tau) \zeta_{f}(f_{s}-f) e^{j(\theta_{s}-\theta)}$$



$$\boldsymbol{\eta}_{\mathrm{a}} = \left[\; \tau_{\mathrm{a}} \; , \; \theta_{\mathrm{a}} \; , \; f_{\mathrm{a}} \; \right]^{\mathsf{T}} \; \mathrm{and} \; \boldsymbol{\eta}_{\mathrm{s}} = \left[\; \tau_{\mathrm{s}} \; , \; \theta_{\mathrm{s}} \; , \; f_{\mathrm{s}} \; \right]^{\mathsf{T}}$$





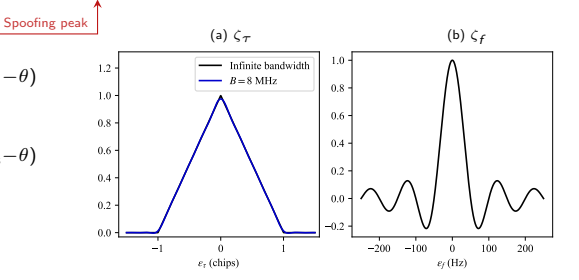
$$\Lambda(\eta, \eta_{\mathsf{a}}, \eta_{\mathsf{s}}) = \Lambda_{\mathsf{a}}(\eta_{\mathsf{a}} - \eta) + \Lambda_{\mathsf{s}}(\eta_{\mathsf{s}} - \eta) + \Lambda_{\chi} + \Lambda_{\eta}$$

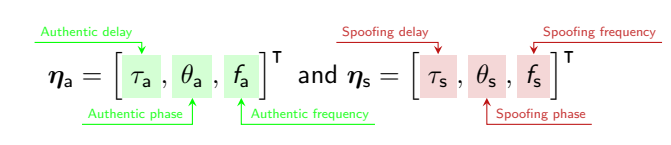
Authentic peak:

$$\Lambda_{a}(\eta_{a}-\eta) = \sqrt{C_{a}} d_{k} \zeta_{\tau}(\tau_{a}-\tau) \zeta_{f}(f_{a}-f) e^{j(\theta_{a}-\theta)}$$

Spoofing peak:

$$\Lambda_{s}(\eta_{s}-\eta) = \sqrt{C_{s}} d_{k} \zeta_{\tau}(\tau_{s}-\tau) \zeta_{f}(f_{s}-f) e^{j(\theta_{s}-\theta)}$$









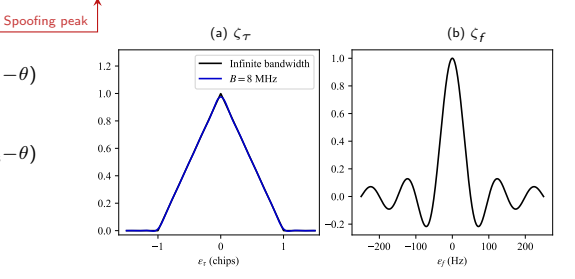
$$\Lambda(\eta,\eta_{\mathsf{a}},\eta_{\mathsf{s}}) = \Lambda_{\mathsf{a}}(\eta_{\mathsf{a}}-\eta) + \Lambda_{\mathsf{s}}(\eta_{\mathsf{s}}-\eta) + \Lambda_{\chi} + \Lambda_{n}$$

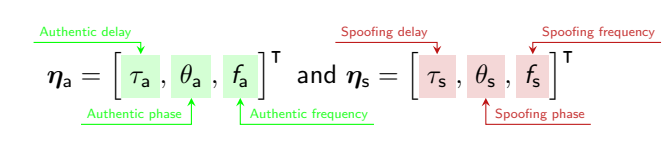
Authentic peak:

$$\Lambda_{\rm a}(\eta_{\rm a}\!-\!\eta) = \sqrt{C_{\rm a}}\,d_k\,\zeta_\tau(\tau_{\rm a}\!-\!\tau)\,\zeta_f(f_{\rm a}\!-\!f)\,e^{j(\theta_{\rm a}-\theta)}$$

Spoofing peak:

$$\Lambda_{s}(\eta_{s}-\eta) = \sqrt{C_{s}} d_{k} \zeta_{\tau}(\tau_{s}-\tau) \zeta_{f}(f_{s}-f) e^{j(\theta_{s}-\theta)}$$









$$\Lambda(\eta,\eta_{\mathsf{a}},\eta_{\mathsf{s}}) = \Lambda_{\mathsf{a}}(\eta_{\mathsf{a}}-\eta) + \Lambda_{\mathsf{s}}(\eta_{\mathsf{s}}-\eta) + \Lambda_{\mathsf{s}}$$

Authentic peak:

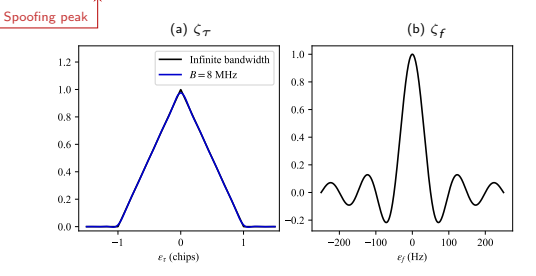
$$\Lambda_{\rm a}(\eta_{\rm a}\!-\!\eta) = \sqrt{C_{\rm a}}\,d_k\,\zeta_\tau(\tau_{\rm a}\!-\!\tau)\,\zeta_f(f_{\rm a}\!-\!f)\,e^{j(\theta_{\rm a}-\theta)}$$

Spoofing peak:

$$\Lambda_{s}(\eta_{s}-\eta) = \sqrt{C_{s}} d_{k} \zeta_{\tau}(\tau_{s}-\tau) \zeta_{f}(f_{s}-f) e^{j(\theta_{s}-\theta)}$$

Random contribution:

$$\Lambda_{\varsigma} = \Lambda_{\chi} + \Lambda_{n} \left(\Lambda_{\varsigma} \sim \mathcal{CN} \left(0, P_{\chi} + P_{n} \right) \right)$$



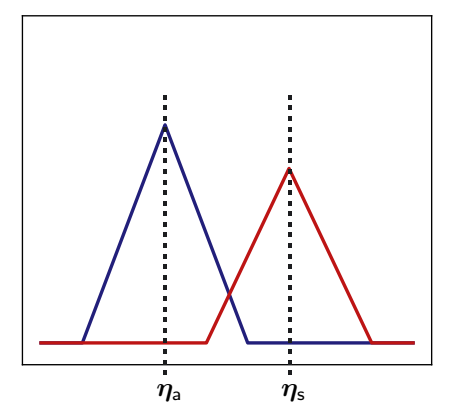






Relative dynamic

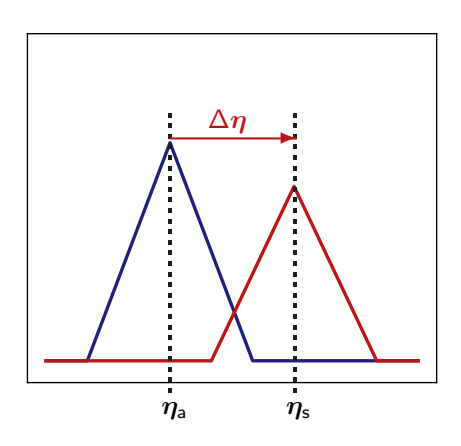
$$\Lambda(\eta, |\eta_{\mathsf{a}}|, |\eta_{\mathsf{s}}|) = \Lambda_{\mathsf{a}}(|\eta_{\mathsf{a}}| - \eta) + \Lambda_{\mathsf{s}}(|\eta_{\mathsf{s}}| - \eta) + \Lambda_{\mathsf{s}}$$







$$\begin{array}{c} \stackrel{\text{Authentic dynamic}}{\searrow} \\ \Lambda(\boldsymbol{\eta}, \ \boldsymbol{\eta_{\mathsf{a}}} \ , \ \Delta\nu \) = \Lambda_{\mathsf{a}}(\ \boldsymbol{\eta_{\mathsf{a}}} \ - \boldsymbol{\eta}) + \ \sqrt{\Delta g} \ \Lambda_{\mathsf{a}}(\ \boldsymbol{\eta_{\mathsf{a}}} \ - \boldsymbol{\eta} + \ \Delta\boldsymbol{\eta} \) + \Lambda_{\varsigma} \end{array}$$



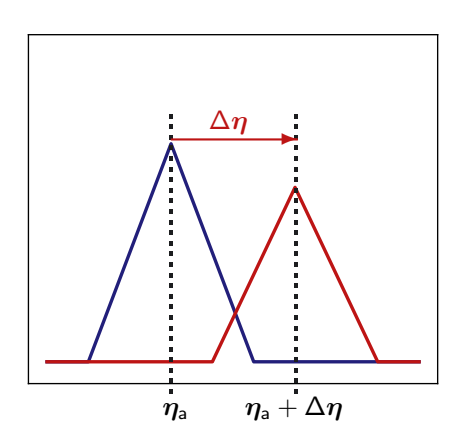
Relative dynamic:







$$\Lambda(\boldsymbol{\eta}, \ \boldsymbol{\eta_{\mathsf{a}}} \ , \ \Delta\nu \) = \Lambda_{\mathsf{a}}(\ \boldsymbol{\eta_{\mathsf{a}}} \ - \boldsymbol{\eta}) + \ \sqrt{\Delta g} \ \Lambda_{\mathsf{a}}(\ \boldsymbol{\eta_{\mathsf{a}}} \ - \boldsymbol{\eta} + \ \Delta\boldsymbol{\eta} \) + \Lambda_{\varsigma}$$



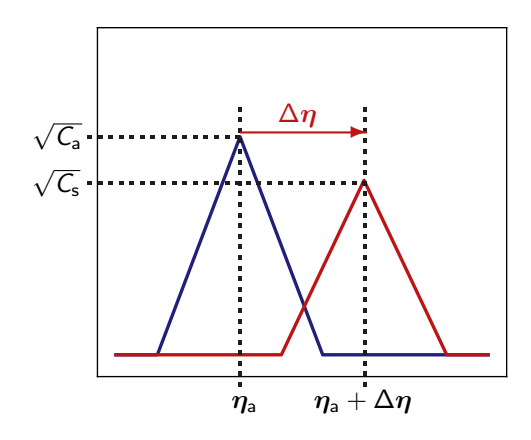
Relative dynamic:

$$\Delta oldsymbol{\eta} = oldsymbol{\eta}_{\mathsf{s}} - oldsymbol{\eta}_{\mathsf{a}} = \left[egin{array}{c} \operatorname{\mathsf{N}}_{\mathsf{d}} & \operatorname{\mathsf{N}}_{\mathsf{d}} & \operatorname{\mathsf{N}}_{\mathsf{d}} \\ \Delta oldsymbol{ heta} & \operatorname{\mathsf{N}}_{\mathsf{d}} & \operatorname{\mathsf{N}}_{\mathsf{d}} & \operatorname{\mathsf{N}}_{\mathsf{d}} \end{array}
ight]^{\mathsf{T}}$$





$$\Lambda(\eta,\;\eta_{\mathsf{a}}\;,\;\Delta
u\;) = \Lambda_{\mathsf{a}}(\;\eta_{\mathsf{a}}\;-\eta) + \;\sqrt{\Delta g}\;\Lambda_{\mathsf{a}}(\;\eta_{\mathsf{a}}\;-\eta + \frac{\Lambda_{\mathsf{a}}(\mathsf{a})}{\Delta\eta}\;) + \Lambda_{\varsigma}$$



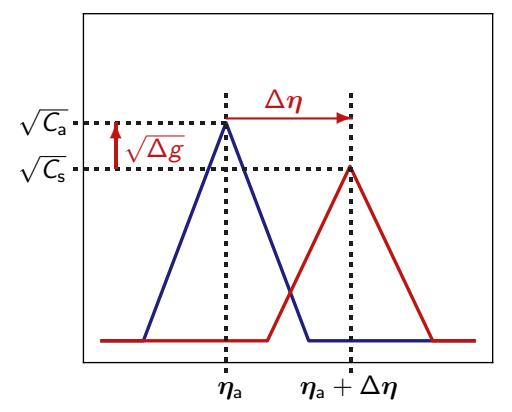
Relative dynamic:







$$\Lambda(\eta, |\eta_{\mathsf{a}}|, |\Delta \nu|) = \Lambda_{\mathsf{a}}(|\eta_{\mathsf{a}}| - \eta) + \sqrt{\Delta g} \Lambda_{\mathsf{a}}(|\eta_{\mathsf{a}}| - \eta + |\Delta \eta|) + \Lambda_{\varsigma}$$



Relative dynamic:

$$\Delta oldsymbol{\eta} = oldsymbol{\eta}_{\mathsf{s}} - oldsymbol{\eta}_{\mathsf{a}} = \left[egin{array}{c} \operatorname{ ext{Relative phase}} \\ \Delta au, & \Delta heta, & \Delta heta \end{array}
ight]^{\mathsf{T}}$$

Relative parameters:

$$\Delta
u = \left[\Delta \eta^{\mathsf{T}}, \Delta g \right]^{\mathsf{T}} \text{ with } \Delta g = C_{\mathsf{s}}/C_{\mathsf{a}}$$





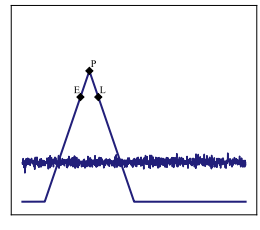
$$\Lambda(\eta,\eta_{\mathsf{a}},\Delta\nu) = \Lambda_{\mathsf{a}}(\eta_{\mathsf{a}}-\eta) + \Lambda_{\mathsf{s}}(\eta_{\mathsf{a}}-\eta,\Delta\nu) +$$





Classification

$$\Lambda(oldsymbol{\eta}, oldsymbol{\eta}_{\mathsf{a}}, \Delta
u) = egin{pmatrix} \Lambda_{\mathsf{a}}(oldsymbol{\eta}_{\mathsf{a}} - oldsymbol{\eta}) \\ + oldsymbol{\Lambda}_{\mathsf{s}}(oldsymbol{\eta}_{\mathsf{a}} - oldsymbol{\eta}, \Delta
u) \end{bmatrix} + oldsymbol{\Lambda}_{\mathsf{s}}(oldsymbol{\eta}_{\mathsf{a}} - oldsymbol{\eta}, \Delta
u)$$



Nominal

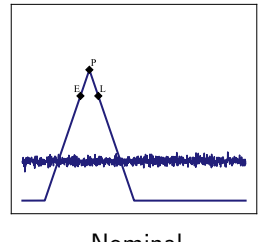
$$\Lambda^{(N)} = \Lambda_a + \Lambda_\varsigma$$

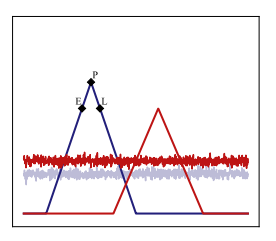




20 / 51

$$\Lambda(\eta,\eta_{\mathsf{a}},\Delta
u) = \Lambda_{\mathsf{a}}(\eta_{\mathsf{a}}-\eta) + \Lambda_{\mathsf{s}}(\eta_{\mathsf{a}}-\eta,\Delta
u) + \Lambda_{\mathsf{c}}$$





Nominal

Induced-jamming

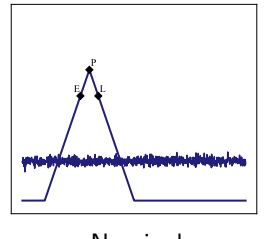
$$\Lambda^{(N)} = \Lambda_a + \Lambda_\varsigma$$

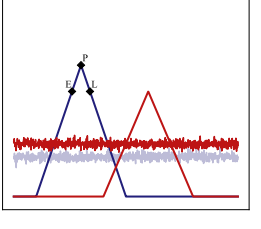
$$\Lambda^{(\mathsf{J})} = |\Lambda_\mathsf{a}| + |\Lambda_\varsigma|$$

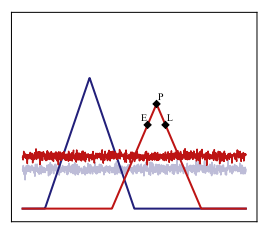




$$\Lambda(\boldsymbol{\eta},\boldsymbol{\eta}_{\mathsf{a}},\Delta\nu) = \Lambda_{\mathsf{a}}(\boldsymbol{\eta}_{\mathsf{a}}-\boldsymbol{\eta}) + \frac{\mathsf{Spoofing peak}}{\mathsf{N}_{\mathsf{s}}(\boldsymbol{\eta}_{\mathsf{a}}-\boldsymbol{\eta},\Delta\nu)} + \Lambda_{\varsigma}$$







Nominal

Induced-jamming

Induced-spoofing

$$\Lambda^{(N)} = \Lambda_a + \Lambda_\varsigma$$

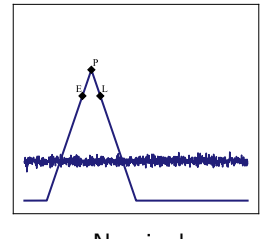
$$\Lambda^{(J)} = \Lambda_a + \Lambda_{\varsigma}$$
 $\Lambda^{(S)} = \Lambda_s + \Lambda_{\varsigma}$

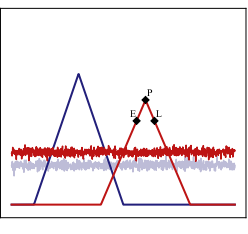
$$\Lambda^{(\mathsf{S})} = oldsymbol{\mathsf{\Lambda}_\mathsf{s}} + oldsymbol{\mathsf{\Lambda}_\mathsf{s}}$$

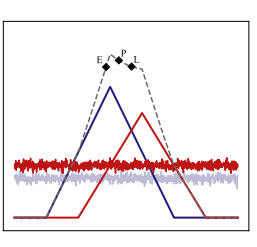




$$\Lambda(\eta,\eta_{\mathsf{a}},\Delta
u) = \Lambda_{\mathsf{a}}(\eta_{\mathsf{a}}-\eta) + \Lambda_{\mathsf{s}}(\eta_{\mathsf{a}}-\eta,\Delta
u) + \Lambda_{\mathsf{s}}(\eta_{\mathsf{a}}-\eta,\Delta
u) + \Lambda_{\mathsf{s}}(\eta_{\mathsf{a}}-\eta,\Delta
u)$$







Nominal

Induced-jamming

Induced-spoofing

Induced-multipath

$$\Lambda^{(N)} = \Lambda_a + \Lambda_{\varsigma}$$

$$\Lambda^{(J)} = \Lambda_a + \Lambda_{\varsigma}$$

$$\Lambda^{(S)} = \Lambda_s + \Lambda_s$$

$$\Lambda^{(S)} = \frac{\Lambda_s}{\Lambda_s} + \Lambda_{\varsigma}$$
 $\Lambda^{(M)} = \Lambda_a + \frac{\Lambda_s}{\Lambda_s} + \Lambda_{\varsigma}$





Outline

- Context
- 2 Received signal model under spoofing
- 3 Impact of spoofing before correlation
- 4 Impact of spoofing after correlation

 Correlator output

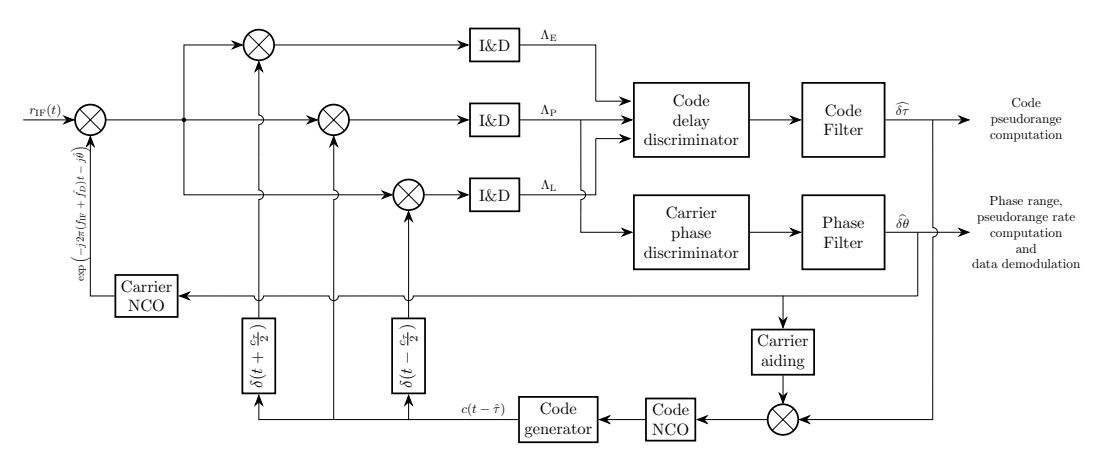
 Tracking loops

 C/N₀
- **5** Experimentation
- **6** Conclusion



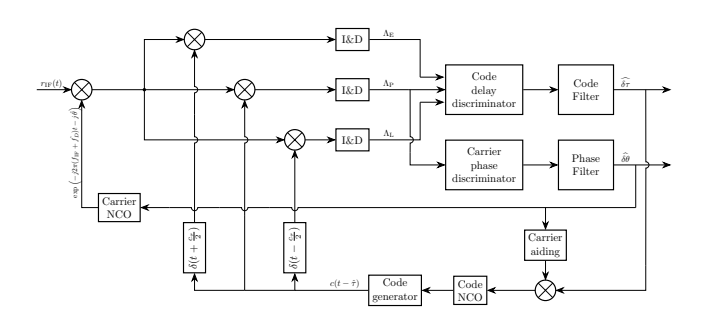


21 / 51





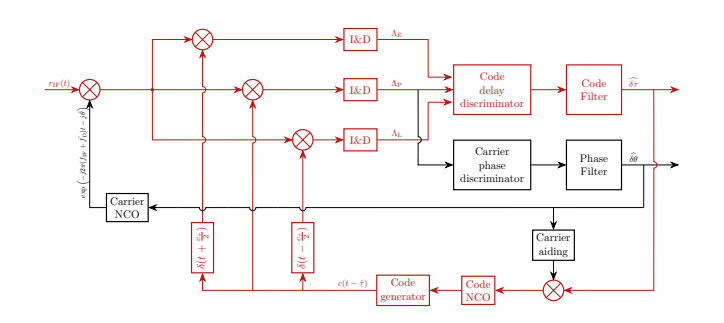








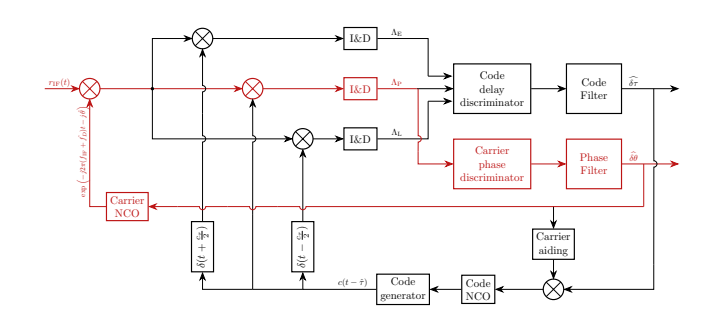
$$\begin{cases} \hat{\tau}(z) + \beta \, \hat{\theta}(z) = \frac{z^{-1}}{1 - z^{-1}} T_{i} F_{\tau}(z) D_{\tau} \left(\eta_{a}(z) - \hat{\eta}(z), \Delta \nu(z) \right) \\ \hat{\theta}(z) = \frac{z^{-1}}{1 - z^{-1}} T_{i} F_{\theta}(z) D_{\theta} \left(\eta_{a}(z) - \hat{\eta}(z), \Delta \nu(z) \right) \end{cases}$$
(DLL)







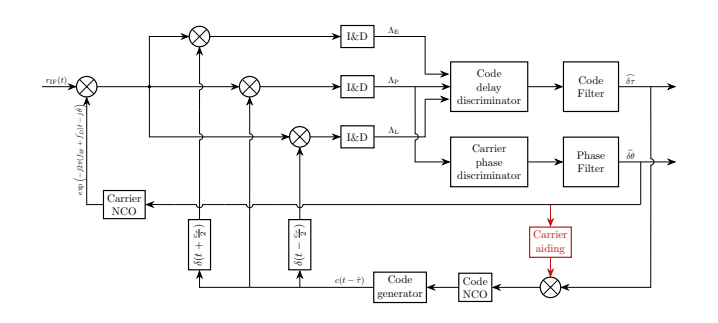
$$\begin{cases} \hat{\tau}(z) + \beta \, \hat{\theta}(z) = \frac{z^{-1}}{1 - z^{-1}} \, T_{\mathrm{i}} \, F_{\tau}(z) \, D_{\tau} \left(\eta_{\mathrm{a}}(z) - \hat{\eta}(z), \Delta \nu(z) \right) \\ \\ \hat{\theta}(z) = \frac{z^{-1}}{1 - z^{-1}} \, T_{\mathrm{i}} \, F_{\theta}(z) \, D_{\theta} \left(\eta_{\mathrm{a}}(z) - \hat{\eta}(z), \Delta \nu(z) \right) \end{cases}$$
(PLL)







$$\begin{cases} \hat{\tau}(z) + \beta \, \hat{\theta}(z) = \frac{z^{-1}}{1 - z^{-1}} \, T_{\mathrm{i}} \, F_{\tau}(z) \, D_{\tau} \left(\eta_{\mathrm{a}}(z) - \hat{\eta}(z), \Delta \nu(z) \right) \\ \hat{\theta}(z) = \frac{z^{-1}}{1 - z^{-1}} \, T_{\mathrm{i}} \, F_{\theta}(z) \, D_{\theta} \left(\eta_{\mathrm{a}}(z) - \hat{\eta}(z), \Delta \nu(z) \right) \end{cases}$$
(PLL)







$$\begin{cases} \hat{\tau}(z) + \beta \ \hat{\theta}(z) = \frac{z^{-1}}{1 - z^{-1}} T_{i} F_{\tau}(z) D_{\tau} \left(\eta_{a}(z) - \hat{\eta}(z), \Delta \nu(z) \right) \\ \hat{\theta}(z) = \frac{z^{-1}}{1 - z^{-1}} T_{i} F_{\theta}(z) D_{\theta} \left(\eta_{a}(z) - \hat{\eta}(z), \Delta \nu(z) \right) \end{cases}$$
(PLL)





$$\begin{cases} \hat{\tau}(z) + \beta \hat{\theta}(z) = \frac{z^{-1}}{1 - z^{-1}} T_{i} F_{\tau}(z) D_{\tau} \left(\eta_{a}(z) - \hat{\eta}(z), \Delta \nu(z) \right) \\ \hat{\theta}(z) = \frac{z^{-1}}{1 - z^{-1}} T_{i} F_{\theta}(z) D_{\theta} \left(\eta_{a}(z) - \hat{\eta}(z), \Delta \nu(z) \right) \end{cases}$$
(DLL)





$$\begin{cases} \hat{\boldsymbol{\tau}}(z) + \beta & \hat{\boldsymbol{\theta}}(z) = \frac{z^{-1}}{1 - z^{-1}} T_{i} F_{\tau}(z) D_{\tau} \left(\boldsymbol{\eta}_{a}(z) - \hat{\boldsymbol{\eta}}(z), \Delta \boldsymbol{\nu}(z) \right) \\ \hat{\boldsymbol{\theta}}(z) = \frac{z^{-1}}{1 - z^{-1}} T_{i} F_{\theta}(z) D_{\theta} \left(\boldsymbol{\eta}_{a}(z) - \hat{\boldsymbol{\eta}}(z), \Delta \boldsymbol{\nu}(z) \right) \end{cases}$$
(PLL)





22 / 51

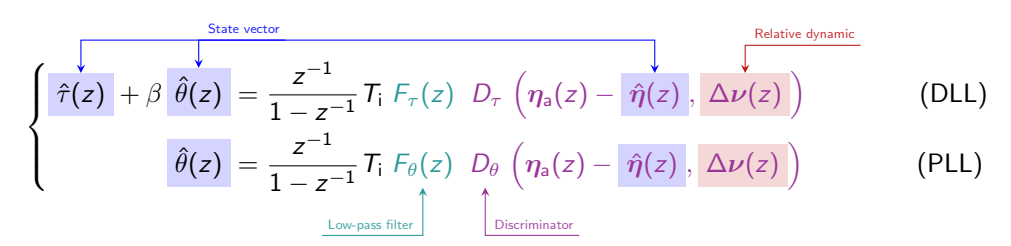
$$\begin{cases} \hat{\tau}(z) + \beta \hat{\theta}(z) = \frac{z^{-1}}{1 - z^{-1}} T_{i} F_{\tau}(z) D_{\tau} \left(\eta_{a}(z) - \hat{\eta}(z), \Delta \nu(z) \right) \\ \hat{\theta}(z) = \frac{z^{-1}}{1 - z^{-1}} T_{i} F_{\theta}(z) D_{\theta} \left(\eta_{a}(z) - \hat{\eta}(z), \Delta \nu(z) \right) \end{cases}$$

$$(DLL)$$

$$\downarrow \text{Low-pass filter} \qquad \downarrow \text{Discriminator}$$





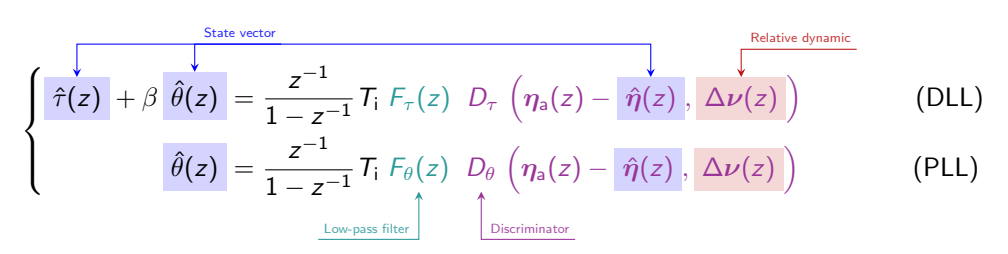






text Received signal Pre-correlator Post-correlator Experimentation Conclusion

Tracking loops model



Dynamic approach:

- Characterize the dynamic behavior under spoofing through the analysis of the closed-loop model.
- Account for the interconnection between DLL and PLL, incorporating all dynamic aspects (e.g., filter and feedback architecture).
- Propose an analysis of linearity, Stable Equilibria (SE), and stochastic behavior for each spoofing-induced situation.





Linearity

Definition: State variable $\hat{\phi}$ and its derivatives appear linearly. A linear system satisfies additivity and homogeneity and can be analyzed though tranfer function tools.¹





Linearity

Definition: State variable $\hat{\phi}$ and its derivatives appear linearly. A linear system satisfies additivity and homogeneity and can be analyzed though tranfer function tools.¹

$$\begin{cases} \hat{\tau}(z) + \beta \hat{\theta}(z) = \frac{z^{-1}}{1 - z^{-1}} T_{i} F_{\tau}(z) D_{\tau} \left(\eta_{a}(z) - \hat{\eta}(z), \Delta \nu(z) \right) \\ \hat{\theta}(z) = \frac{z^{-1}}{1 - z^{-1}} T_{i} F_{\theta}(z) D_{\theta} \left(\eta_{a}(z) - \hat{\eta}(z), \Delta \nu(z) \right) \end{cases}$$

$$(DLL)$$

$$\hat{\theta}(z) = \frac{z^{-1}}{1 - z^{-1}} T_{i} F_{\theta}(z) D_{\theta} \left(\eta_{a}(z) - \hat{\eta}(z), \Delta \nu(z) \right)$$

$$(DLL)$$

$$\hat{\theta}(z) = \frac{z^{-1}}{1 - z^{-1}} T_{i} F_{\theta}(z) D_{\theta} \left(\eta_{a}(z) - \hat{\eta}(z), \Delta \nu(z) \right)$$

$$(DLL)$$





Linearity

Definition: State variable $\hat{\phi}$ and its derivatives appear linearly. A linear system satisfies additivity and homogeneity and can be analyzed though tranfer function tools.¹

$$\begin{cases} \hat{\tau}(z) + \beta \hat{\theta}(z) = \frac{z^{-1}}{1 - z^{-1}} T_{i} F_{\tau}(z) D_{\tau} \left(\eta_{a}(z) - \hat{\eta}(z), \Delta \nu(z) \right) \\ \hat{\theta}(z) = \frac{z^{-1}}{1 - z^{-1}} T_{i} F_{\theta}(z) D_{\theta} \left(\eta_{a}(z) - \hat{\eta}(z), \Delta \nu(z) \right) \end{cases}$$

$$(DLL)$$

$$\hat{\theta}(z) = \frac{z^{-1}}{1 - z^{-1}} T_{i} F_{\theta}(z) D_{\theta} \left(\eta_{a}(z) - \hat{\eta}(z), \Delta \nu(z) \right)$$

$$(DLL)$$

$$\hat{\theta}(z) = \frac{z^{-1}}{1 - z^{-1}} T_{i} F_{\theta}(z) D_{\theta} \left(\eta_{a}(z) - \hat{\eta}(z), \Delta \nu(z) \right)$$

$$(DLL)$$

Results

- √ Maintains its linearity assumption under induced jamming and spoofing situations (near SE).
- × Exhibits non-linearity in both DLL and PLL under induced multipath situation.





¹Floyd M Gardner. *Phaselock Techniques*. John Wiley & Sons, 2005

Stable Equilibria (SE) (1/3)

Stable Equilibrium: State where the system has successfully converged and returns to this state after a small perturbation.¹





¹Gennady A. Leonov et al. "Hold-In, Pull-In, and Lock-In Ranges of PLL Circuits: Rigorous Mathematical Definitions and Limitations of Classical Theory". In: IEEE Trans. Circuits Syst. I. Reg. Papers 62.10 (2015), pp. 2454–2464

Received signal Pre-correlator Post-correlator Experimentation Conclus

Stable Equilibria (SE) (1/3)

Stable Equilibrium: State where the system has successfully converged and returns to this state after a small perturbation. 1

Objective

- Enable the analysis of system convergence (identifying the different points of convergence and potential bifurcations).
- Facilitate the analysis of the **system's dynamic behavior**, including transient response, tracking error at lock, and stress error.





¹Gennady A. Leonov et al. "Hold-In, Pull-In, and Lock-In Ranges of PLL Circuits: Rigorous Mathematical Definitions and Limitations of Classical Theory". In: IEEE Trans. Circuits Syst. I. Res. Papers 62.10 (2015), pp. 2454–2464

Stable Equilibria (SE) (1/3)

Stable Equilibrium: State where the system has successfully converged and returns to this state after a small perturbation.¹

Objective

- Enable the analysis of system convergence (identifying the different points of convergence and potential bifurcations).
- Facilitate the analysis of the system's dynamic behavior, including transient response, tracking error at lock, and stress error.

Closed-loop model SE:

$$\begin{cases} d_{\tau} \left(\varepsilon_{\eta}^{I}, \Delta \nu \right) = 0, & d_{\theta} \left(\varepsilon_{\eta}^{I}, \Delta \nu \right) = 0, & \chi_{f} \left(\varepsilon_{\eta}^{I}, \Delta \nu \right) = 0 & \text{(Equilibrium)} \\ \frac{\partial}{\partial \varepsilon_{\tau}} \left(\varepsilon_{\eta}^{I}, \Delta \nu \right) = 0, & \frac{\partial}{\partial \varepsilon_{\theta}} \left(\varepsilon_{\eta}^{I}, \Delta \nu \right) = 0, & \frac{\partial}{\partial \varepsilon_{f}} \left(\varepsilon_{\eta}^{I}, \Delta \nu \right) = 0 & \text{(Stability)} \\ \frac{\partial}{\partial \varepsilon_{\tau}} \left(\varepsilon_{\eta}^{I}, \Delta \nu \right) = 0, & \frac{\partial}{\partial \varepsilon_{\theta}} \left(\varepsilon_{\eta}^{I}, \Delta \nu \right) = 0, & \frac{\partial}{\partial \varepsilon_{\theta}} \left(\varepsilon_{\eta}^{I}, \Delta \nu \right) = 0 & \text{(Stability)} \\ \frac{\partial}{\partial \varepsilon_{\tau}} \left(\varepsilon_{\eta}^{I}, \Delta \nu \right) = 0, & \frac{\partial}{\partial \varepsilon_{\theta}} \left(\varepsilon_{\eta}^{I}, \Delta \nu \right) = 0, & \frac{\partial}{\partial \varepsilon_{\theta}} \left(\varepsilon_{\eta}^{I}, \Delta \nu \right) = 0, & \frac{\partial}{\partial \varepsilon_{\theta}} \left(\varepsilon_{\eta}^{I}, \Delta \nu \right) = 0, & \frac{\partial}{\partial \varepsilon_{\theta}} \left(\varepsilon_{\eta}^{I}, \Delta \nu \right) = 0, & \frac{\partial}{\partial \varepsilon_{\theta}} \left(\varepsilon_{\eta}^{I}, \Delta \nu \right) = 0, & \frac{\partial}{\partial \varepsilon_{\theta}} \left(\varepsilon_{\eta}^{I}, \Delta \nu \right) = 0, & \frac{\partial}{\partial \varepsilon_{\theta}} \left(\varepsilon_{\eta}^{I}, \Delta \nu \right) = 0, & \frac{\partial}{\partial \varepsilon_{\theta}} \left(\varepsilon_{\eta}^{I}, \Delta \nu \right) = 0, & \frac{\partial}{\partial \varepsilon_{\theta}} \left(\varepsilon_{\eta}^{I}, \Delta \nu \right) = 0, & \frac{\partial}{\partial \varepsilon_{\theta}} \left(\varepsilon_{\eta}^{I}, \Delta \nu \right) = 0, & \frac{\partial}{\partial \varepsilon_{\theta}} \left(\varepsilon_{\eta}^{I}, \Delta \nu \right) = 0, & \frac{\partial}{\partial \varepsilon_{\theta}} \left(\varepsilon_{\eta}^{I}, \Delta \nu \right) = 0, & \frac{\partial}{\partial \varepsilon_{\theta}} \left(\varepsilon_{\eta}^{I}, \Delta \nu \right) = 0, & \frac{\partial}{\partial \varepsilon_{\theta}} \left(\varepsilon_{\eta}^{I}, \Delta \nu \right) = 0, & \frac{\partial}{\partial \varepsilon_{\theta}} \left(\varepsilon_{\eta}^{I}, \Delta \nu \right) = 0, & \frac{\partial}{\partial \varepsilon_{\theta}} \left(\varepsilon_{\eta}^{I}, \Delta \nu \right) = 0, & \frac{\partial}{\partial \varepsilon_{\theta}} \left(\varepsilon_{\eta}^{I}, \Delta \nu \right) = 0, & \frac{\partial}{\partial \varepsilon_{\theta}} \left(\varepsilon_{\eta}^{I}, \Delta \nu \right) = 0, & \frac{\partial}{\partial \varepsilon_{\theta}} \left(\varepsilon_{\eta}^{I}, \Delta \nu \right) = 0, & \frac{\partial}{\partial \varepsilon_{\theta}} \left(\varepsilon_{\eta}^{I}, \Delta \nu \right) = 0, & \frac{\partial}{\partial \varepsilon_{\theta}} \left(\varepsilon_{\eta}^{I}, \Delta \nu \right) = 0, & \frac{\partial}{\partial \varepsilon_{\theta}} \left(\varepsilon_{\eta}^{I}, \Delta \nu \right) = 0, & \frac{\partial}{\partial \varepsilon_{\theta}} \left(\varepsilon_{\eta}^{I}, \Delta \nu \right) = 0, & \frac{\partial}{\partial \varepsilon_{\theta}} \left(\varepsilon_{\eta}^{I}, \Delta \nu \right) = 0, & \frac{\partial}{\partial \varepsilon_{\theta}} \left(\varepsilon_{\eta}^{I}, \Delta \nu \right) = 0, & \frac{\partial}{\partial \varepsilon_{\theta}} \left(\varepsilon_{\eta}^{I}, \Delta \nu \right) = 0, & \frac{\partial}{\partial \varepsilon_{\theta}} \left(\varepsilon_{\eta}^{I}, \Delta \nu \right) = 0, & \frac{\partial}{\partial \varepsilon_{\theta}} \left(\varepsilon_{\eta}^{I}, \Delta \nu \right) = 0, & \frac{\partial}{\partial \varepsilon_{\theta}} \left(\varepsilon_{\eta}^{I}, \Delta \nu \right) = 0, & \frac{\partial}{\partial \varepsilon_{\theta}} \left(\varepsilon_{\eta}^{I}, \Delta \nu \right) = 0, & \frac{\partial}{\partial \varepsilon_{\theta}} \left(\varepsilon_{\eta}^{I}, \Delta \nu \right) = 0, & \frac{\partial}{\partial \varepsilon_{\theta}} \left(\varepsilon_{\eta}^{I}, \Delta \nu \right) = 0, & \frac{\partial}{\partial \varepsilon_{\theta}} \left(\varepsilon_{\eta}^{I}, \Delta \nu \right) = 0, & \frac{\partial}{\partial \varepsilon_{\theta}} \left(\varepsilon_{\eta}^{I}, \Delta \nu \right) = 0, & \frac{\partial}{\partial \varepsilon_{\theta}} \left(\varepsilon_{\eta}^{I}, \Delta \nu \right) = 0, & \frac{\partial}{\partial \varepsilon_{\theta}} \left(\varepsilon_{\eta}^{I}, \Delta \nu \right) = 0, & \frac{\partial}{\partial \varepsilon_{\theta}} \left(\varepsilon_{\eta}^{I}, \Delta \nu \right) = 0, & \frac{\partial}{\partial \varepsilon_{\theta}} \left(\varepsilon_{\eta}^{I}, \Delta \nu \right) = 0, &$$

¹Gennady A. Leonov et al. "Hold-In, Pull-In, and Lock-In Ranges of PLL Circuits: Rigorous Mathematical Definitions and Limitations of Classical Theory". In: IEEE Trans. Circuits Syst. I. Res. Papers 62.10 (2015), pp. 2454–2464



Stable Equilibria (SE) (1/3)

Stable Equilibrium: State where the system has successfully converged and returns to this state after a small perturbation.¹

Objective

- Enable the analysis of system convergence (identifying the different points of convergence and potential bifurcations).
- Facilitate the analysis of the **system's dynamic behavior**, including transient response. tracking error at lock, and stress error.

Closed-loop model SE:

$$\begin{cases} d_{\tau} \left(\varepsilon_{\eta}^{I}, \Delta \nu \right) = 0, & d_{\theta} \left(\varepsilon_{\eta}^{I}, \Delta \nu \right) = 0, \\ \frac{\partial}{\partial \varepsilon_{\tau}} \left(\varepsilon_{\eta}^{I}, \Delta \nu \right) = 0, & \frac{\partial}{\partial \varepsilon_{\theta}} \left(\varepsilon_{\eta}^{I}, \Delta \nu \right) = 0, \\ \frac{\partial}{\partial \varepsilon_{\tau}} \left(\varepsilon_{\eta}^{I}, \Delta \nu \right) = 0, & \frac{\partial}{\partial \varepsilon_{\theta}} \left(\varepsilon_{\eta}^{I}, \Delta \nu \right) = 0, \\ \frac{\partial}{\partial \varepsilon_{\tau}} \left(\varepsilon_{\eta}^{I}, \Delta \nu \right) = 0, & \frac{\partial}{\partial \varepsilon_{\theta}} \left(\varepsilon_{\eta}^{I}, \Delta \nu \right) = 0, \\ \frac{\partial}{\partial \varepsilon_{\tau}} \left(\varepsilon_{\eta}^{I}, \Delta \nu \right) = 0, & \frac{\partial}{\partial \varepsilon_{\theta}} \left(\varepsilon_{\eta}^{I}, \Delta \nu \right) = 0, \\ \frac{\partial}{\partial \varepsilon_{\tau}} \left(\varepsilon_{\eta}^{I}, \Delta \nu \right) = 0, & \frac{\partial}{\partial \varepsilon_{\theta}} \left(\varepsilon_{\eta}^{I}, \Delta \nu \right) = 0, \\ \frac{\partial}{\partial \varepsilon_{\tau}} \left(\varepsilon_{\eta}^{I}, \Delta \nu \right) = 0, & \frac{\partial}{\partial \varepsilon_{\theta}} \left(\varepsilon_{\eta}^{I}, \Delta \nu \right) = 0, \\ \frac{\partial}{\partial \varepsilon_{\tau}} \left(\varepsilon_{\eta}^{I}, \Delta \nu \right) = 0, & \frac{\partial}{\partial \varepsilon_{\theta}} \left(\varepsilon_{\eta}^{I}, \Delta \nu \right) = 0, \\ \frac{\partial}{\partial \varepsilon_{\tau}} \left(\varepsilon_{\eta}^{I}, \Delta \nu \right) = 0, & \frac{\partial}{\partial \varepsilon_{\theta}} \left(\varepsilon_{\eta}^{I}, \Delta \nu \right) = 0, \\ \frac{\partial}{\partial \varepsilon_{\tau}} \left(\varepsilon_{\eta}^{I}, \Delta \nu \right) = 0, & \frac{\partial}{\partial \varepsilon_{\theta}} \left(\varepsilon_{\eta}^{I}, \Delta \nu \right) = 0, \\ \frac{\partial}{\partial \varepsilon_{\tau}} \left(\varepsilon_{\eta}^{I}, \Delta \nu \right) = 0, & \frac{\partial}{\partial \varepsilon_{\theta}} \left(\varepsilon_{\eta}^{I}, \Delta \nu \right) = 0, \\ \frac{\partial}{\partial \varepsilon_{\tau}} \left(\varepsilon_{\eta}^{I}, \Delta \nu \right) = 0, & \frac{\partial}{\partial \varepsilon_{\theta}} \left(\varepsilon_{\eta}^{I}, \Delta \nu \right) = 0, \\ \frac{\partial}{\partial \varepsilon_{\tau}} \left(\varepsilon_{\eta}^{I}, \Delta \nu \right) = 0, & \frac{\partial}{\partial \varepsilon_{\theta}} \left(\varepsilon_{\eta}^{I}, \Delta \nu \right) = 0, \\ \frac{\partial}{\partial \varepsilon_{\tau}} \left(\varepsilon_{\eta}^{I}, \Delta \nu \right) = 0, & \frac{\partial}{\partial \varepsilon_{\theta}} \left(\varepsilon_{\eta}^{I}, \Delta \nu \right) = 0, \\ \frac{\partial}{\partial \varepsilon_{\tau}} \left(\varepsilon_{\eta}^{I}, \Delta \nu \right) = 0, & \frac{\partial}{\partial \varepsilon_{\theta}} \left(\varepsilon_{\eta}^{I}, \Delta \nu \right) = 0, \\ \frac{\partial}{\partial \varepsilon_{\tau}} \left(\varepsilon_{\eta}^{I}, \Delta \nu \right) = 0, & \frac{\partial}{\partial \varepsilon_{\theta}} \left(\varepsilon_{\eta}^{I}, \Delta \nu \right) = 0, \\ \frac{\partial}{\partial \varepsilon_{\tau}} \left(\varepsilon_{\eta}^{I}, \Delta \nu \right) = 0, & \frac{\partial}{\partial \varepsilon_{\theta}} \left(\varepsilon_{\eta}^{I}, \Delta \nu \right) = 0, \\ \frac{\partial}{\partial \varepsilon_{\tau}} \left(\varepsilon_{\eta}^{I}, \Delta \nu \right) = 0, & \frac{\partial}{\partial \varepsilon_{\theta}} \left(\varepsilon_{\eta}^{I}, \Delta \nu \right) = 0, \\ \frac{\partial}{\partial \varepsilon_{\tau}} \left(\varepsilon_{\eta}^{I}, \Delta \nu \right) = 0, & \frac{\partial}{\partial \varepsilon_{\tau}} \left(\varepsilon_{\eta}^{I}, \Delta \nu \right) = 0, \\ \frac{\partial}{\partial \varepsilon_{\tau}} \left(\varepsilon_{\eta}^{I}, \Delta \nu \right) = 0, & \frac{\partial}{\partial \varepsilon_{\tau}} \left(\varepsilon_{\eta}^{I}, \Delta \nu \right) = 0, \\ \frac{\partial}{\partial \varepsilon_{\tau}} \left(\varepsilon_{\eta}^{I}, \Delta \nu \right) = 0, & \frac{\partial}{\partial \varepsilon_{\tau}} \left(\varepsilon_{\eta}^{I}, \Delta \nu \right) = 0, \\ \frac{\partial}{\partial \varepsilon_{\tau}} \left(\varepsilon_{\eta}^{I}, \Delta \nu \right) = 0, & \frac{\partial}{\partial \varepsilon_{\tau}} \left(\varepsilon_{\eta}^{I}, \Delta \nu \right) = 0, \\ \frac{\partial}{\partial \varepsilon_{\tau}} \left(\varepsilon_{\eta}^{I}, \Delta \nu \right) = 0, & \frac{\partial}{\partial \varepsilon_{\tau}} \left(\varepsilon_{\eta}^{I}, \Delta \nu \right) = 0, \\ \frac{\partial}{\partial \varepsilon_{\tau}} \left(\varepsilon_{\eta}^{I}, \Delta \nu \right) = 0, & \frac{\partial}{\partial \varepsilon_{\tau}} \left(\varepsilon_{\eta}^{I}, \Delta \nu \right) = 0, \\ \frac{\partial}{\partial \varepsilon_{\tau}} \left(\varepsilon_{\eta}^{I}, \Delta \nu \right) = 0, &$$

1 Gennady A. Leonov et al. "Hold-In, Pull-In, and Lock-In Ranges of PLL Circuits: Rigorous Mathematical Definitions and Limitations of Classical Theory". In: IEEE Trans. Circuits Syst. I. Reg. Papers 62.10 (2015), pp. 2454-2464



Stable Equilibria (SE) (1/3)

Stable Equilibrium: State where the system has successfully converged and returns to this state after a small perturbation.¹

Objective

- Enable the analysis of system convergence (identifying the different points of convergence and potential bifurcations).
- Facilitate the analysis of the system's dynamic behavior, including transient response, tracking error at lock, and stress error.

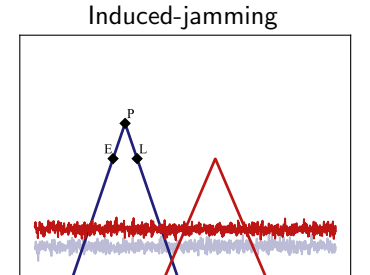
Closed-loop model SE:

 $\begin{cases} d_{\tau}\left(\varepsilon_{\eta}^{I}, \Delta \nu\right) = 0, & d_{\theta}\left(\varepsilon_{\eta}^{I}, \Delta \nu\right) = 0, & \chi_{f}\left(\varepsilon_{\eta}^{I}, \Delta \nu\right) = 0 & \text{(Equilibrium)} \\ \frac{\partial}{\partial \varepsilon_{\tau}}\left(\varepsilon_{\eta}^{I}, \Delta \nu\right) = 0, & \frac{\partial}{\partial \varepsilon_{\theta}}\left(\varepsilon_{\eta}^{I}, \Delta \nu\right) = 0, & \frac{\partial}{\partial \varepsilon_{f}}\left(\varepsilon_{\eta}^{I}, \Delta \nu\right) = 0 & \text{(Stability)} \end{cases}$

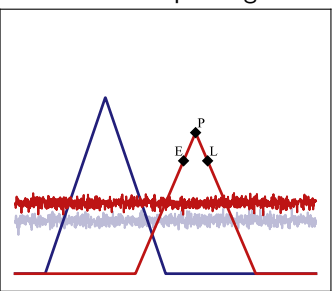
¹Gennady A. Leonov et al. "Hold-In, Pull-In, and Lock-In Ranges of PLL Circuits: Rigorous Mathematical Definitions and Limitations of Classical Theory". In: IEEE Trans. Circuits Syst. I. Reg. Papers 62.10 (2015). pp. 2454–2464



Stable Equilibria (SE) (2/3)



Induced-spoofing



LINEAR ASSUMPTION



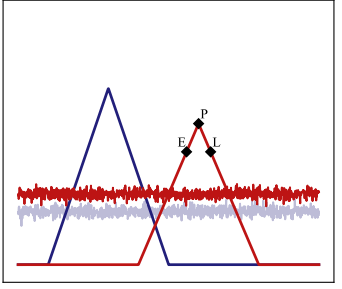


Stable Equilibria (SE) (2/3)

Induced-jamming

Tracked dynamic: Authentic dynamic η_a or frequency-mismatched version $(1/2T_i)$

Induced-spoofing







Stable Equilibria (SE) (2/3)

Induced-jamming

Induced-spoofing

Tracked dynamic: Authentic dynamic η_a or frequency-mismatched version $(1/2T_i)$

Tracked dynamic: Spoofing dynamic η_s or a frequency-mismatched version $(1/2T_i)$





Stable Equilibria (SE) (2/3)

Induced-jamming

Induced-spoofing

Tracked dynamic: Authentic dynamic η_a or frequency-mismatched version $(1/2T_i)$

Tracked dynamic: Spoofing dynamic η_s or a frequency-mismatched version $(1/2T_i)$





Stable Equilibria (SE) (3/3)

System SE under induced-multipath:

$$\begin{cases} d_{\tau}\left(\boldsymbol{\varepsilon}_{\eta}^{l}, \Delta \boldsymbol{\nu}\right) = 0, & d_{\theta}\left(\boldsymbol{\varepsilon}_{\eta}^{l}, \Delta \boldsymbol{\nu}\right) = 0, & \chi_{f}\left(\boldsymbol{\varepsilon}_{\eta}^{l}, \Delta \boldsymbol{\nu}\right) = 0\\ \frac{\partial d_{\tau}\left(\boldsymbol{\varepsilon}_{\eta}^{l}, \Delta \boldsymbol{\nu}\right)}{\partial \varepsilon_{\tau}} > 0, & \frac{\partial d_{\theta}\left(\boldsymbol{\varepsilon}_{\eta}^{l}, \Delta \boldsymbol{\nu}\right)}{\partial \varepsilon_{\theta}} > 0, & \frac{\partial \chi_{f}\left(\boldsymbol{\varepsilon}_{\eta}^{l}, \Delta \boldsymbol{\nu}\right)}{\partial \varepsilon_{f}} > 0 \end{cases}$$

System SE Phase SE
$$\boldsymbol{\varepsilon}_{\eta}^{I} = \begin{bmatrix} \boldsymbol{\varepsilon}_{\tau}{}^{I}, & \boldsymbol{\varepsilon}_{\theta}{}^{I} \end{bmatrix}^{\mathsf{T}}$$
Code SE Frequency SE

A NON-LINEAR AND INTERDEPENDENT A





Stable Equilibria (SE) (3/3)

System SE under induced-multipath:

$$\begin{cases} d_{\tau}\left(\left.\varepsilon_{\tau}^{I},\varepsilon_{f}^{I}\right,\Delta\nu\right)=0, & d_{\theta}\left(\left.\varepsilon_{\eta}^{I}\right,\Delta\nu\right)=0, & \chi_{f}\left(\left.\varepsilon_{\tau}^{I},\varepsilon_{f}^{I}\right,\Delta\nu\right)=0\\ \frac{\partial d_{\tau}\left(\left.\varepsilon_{\tau}^{I},\varepsilon_{f}^{I}\right,\Delta\nu\right)}{\partial\varepsilon_{\tau}}>0, & \frac{\partial d_{\theta}\left(\left.\varepsilon_{\eta}^{I}\right,\Delta\nu\right)}{\partial\varepsilon_{\theta}}>0, & \frac{\partial \chi_{f}\left(\left.\varepsilon_{\tau}^{I},\varepsilon_{f}^{I}\right,\Delta\nu\right)}{\partial\varepsilon_{f}}>0 \end{cases} > 0 \end{cases}$$

$$\boldsymbol{\varepsilon}_{\eta}^{I} = \begin{bmatrix} \boldsymbol{\varepsilon}_{\tau}{}^{I}, \ \boldsymbol{\varepsilon}_{f}{}^{I}, \ \boldsymbol{\varepsilon}_{\theta}{}^{I} \end{bmatrix}^{\mathsf{T}}$$

$$\underline{\mathbf{Code SE}}$$
Frequency SE

 $\mathbf{\Lambda}$ d_{τ} and χ_f INDEPENDENT OF PHASE ERROR $\mathbf{\Lambda}$





Received signal Pre-correlator Post-correlator Experimentation Conclusion

Stable Equilibria (SE) (3/3) System SE under induced-multipath:

$$\begin{cases} d_{\tau}\left(\varepsilon_{\tau}^{l}, \varepsilon_{f}^{l}, \Delta \nu\right) = 0, & d_{\theta}\left(\varepsilon_{\eta}^{l}, \Delta \nu\right) = 0, & \chi_{f}\left(\varepsilon_{\tau}^{l}, \varepsilon_{f}^{l}, \Delta \nu\right) = 0\\ \frac{\partial d_{\tau}\left(\varepsilon_{\tau}^{l}, \varepsilon_{f}^{l}, \Delta \nu\right)}{\partial \varepsilon_{\tau}} > 0, & \frac{\partial d_{\theta}\left(\varepsilon_{\eta}^{l}, \Delta \nu\right)}{\partial \varepsilon_{\theta}} > 0, & \frac{\partial \chi_{f}\left(\varepsilon_{\tau}^{l}, \varepsilon_{f}^{l}, \Delta \nu\right)}{\partial \varepsilon_{f}} > 0 \end{cases}$$

$$\begin{array}{c} \begin{array}{c} \text{System SE} \\ \hline \boldsymbol{\varepsilon}_{\eta}^{\prime} = \begin{bmatrix} \boldsymbol{\varepsilon}_{\tau}^{ \prime}, & \boldsymbol{\varepsilon}_{f}^{ \prime}, & \boldsymbol{\varepsilon}_{\theta}^{ \prime} \end{bmatrix}^{\mathsf{T}} \\ \hline \underline{\boldsymbol{\varepsilon}_{\text{Ode SE}}} & & \\ \hline \end{array}$$

 $\mathbf{\Lambda}$ d_{τ} and χ_f INDEPENDENT OF PHASE ERROR $\mathbf{\Lambda}$





Stable Equilibria (SE) (3/3) System SE under induced-multipath:

$$\begin{cases} d_{\tau}\left(\left[\varepsilon_{\tau}^{l}, \varepsilon_{f}^{l}\right], \Delta\nu\right) = 0, & d_{\theta}\left(\left[\varepsilon_{\eta}^{l}\right], \Delta\nu\right) = 0, & \chi_{f}\left(\left[\varepsilon_{\tau}^{l}, \varepsilon_{f}^{l}\right], \Delta\nu\right) = 0\\ \frac{\partial d_{\tau}\left(\left[\varepsilon_{\tau}^{l}, \varepsilon_{f}^{l}\right], \Delta\nu\right)}{\partial\varepsilon_{\tau}} > 0, & \frac{\partial d_{\theta}\left(\left[\varepsilon_{\eta}^{l}\right], \Delta\nu\right)}{\partial\varepsilon_{\theta}} > 0, & \frac{\partial \chi_{f}\left(\left[\varepsilon_{\tau}^{l}, \varepsilon_{f}^{l}\right], \Delta\nu\right)}{\partial\varepsilon_{f}} > 0. \end{cases}$$

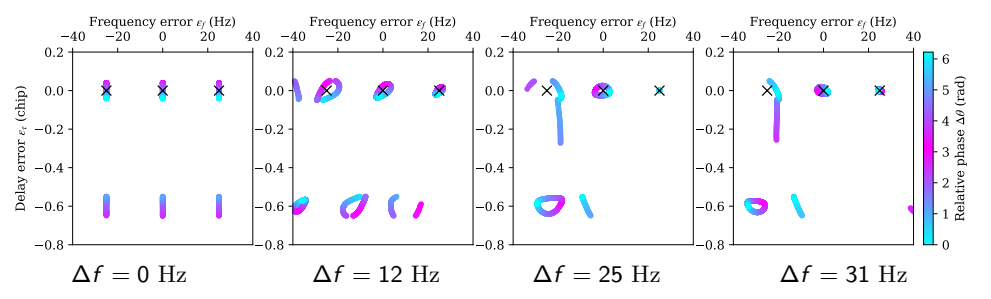
 $oldsymbol{\Lambda}_{\tau}$ and χ_f INDEPENDENT OF PHASE ERROR $oldsymbol{\Lambda}$





Stable Equilibria (SE) (3/3)

System SE under induced-multipath:

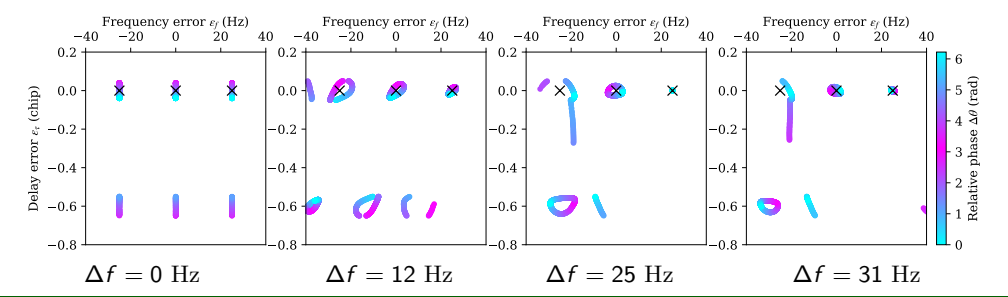






Stable Equilibria (SE) (3/3)

System SE under induced-multipath:

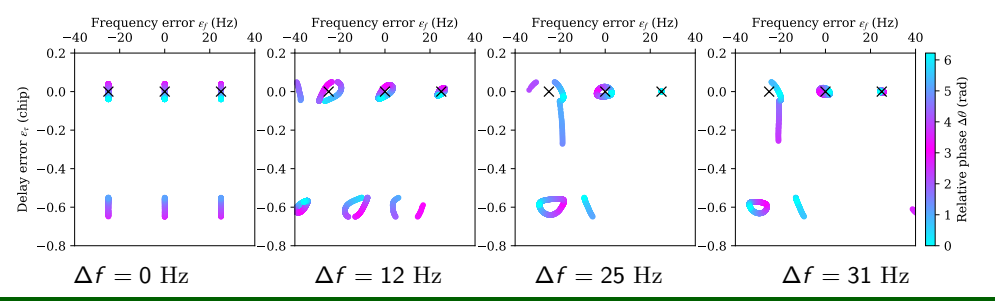


Induced-Multipath Results (Asynchronous Frequency Spoofer)



Stable Equilibria (SE) (3/3)

System SE under induced-multipath:



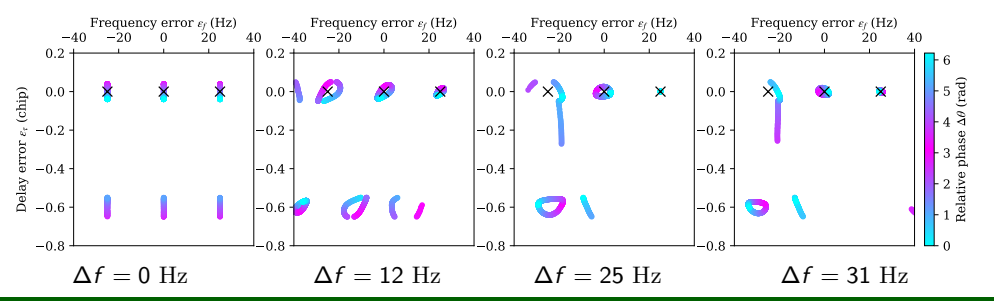
Induced-Multipath Results (Asynchronous Frequency Spoofer)

▲ Emergence of multiple possible points of convergence (chaotic behavior and bifurcations).



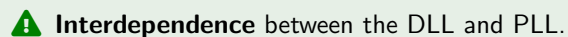
Stable Equilibria (SE) (3/3)

System SE under induced-multipath:



Induced-Multipath Results (Asynchronous Frequency Spoofer)

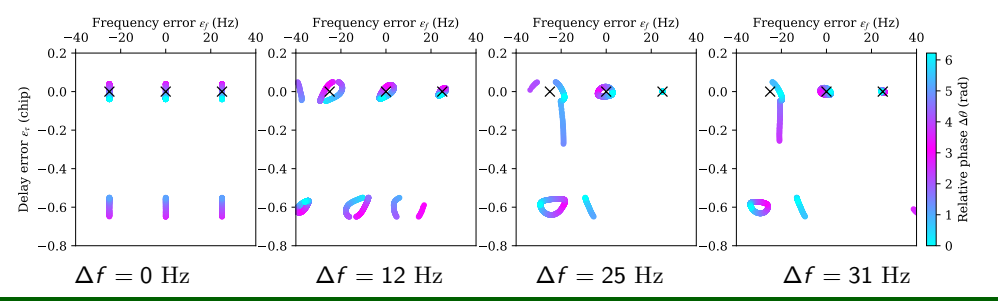
▲ Emergence of multiple possible points of convergence (chaotic behavior and bifurcations).





Stable Equilibria (SE) (3/3)

System SE under induced-multipath:



Induced-Multipath Results (Asynchronous Frequency Spoofer)

▲ Emergence of multiple possible points of convergence (chaotic behavior and bifurcations).

A Interdependence between the DLL and PLL.

A Oscillating patterns over the relative phase $\Delta \theta \in [0, 2\pi]$.



Dynamic and stochastic response (1/5)

Objective

• Characterize the dynamic response of the loops, including transient behavior and all dynamic aspects (feedback and filtering).





Dynamic and stochastic response (1/5)

Objective

- Characterize the dynamic response of the loops, including transient behavior and all dynamic aspects (feedback and filtering).
- Evaluate the **impact of noise** on the dynamic response.¹





Dynamic and stochastic response (1/5)

Objective

- Characterize the dynamic response of the loops, including transient behavior and all dynamic aspects (feedback and filtering).
- Evaluate the impact of noise on the dynamic response.¹

Closed-loop model:

$$\begin{cases} \hat{\tau}(z) + \beta \hat{\theta}(z) = \frac{z^{-1}}{1 - z^{-1}} T_{i} F_{\tau}(z) D_{\tau} \left(\eta_{a}(z) - \hat{\eta}(z), \Delta \nu(z) \right) \\ \hat{\theta}(z) = \frac{z^{-1}}{1 - z^{-1}} T_{i} F_{\theta}(z) D_{\theta} \left(\eta_{a}(z) - \hat{\eta}(z), \Delta \nu(z) \right) \end{cases}$$
(DLL)

$$\hat{\theta}(z) = \frac{z^{-1}}{1 - z^{-1}} T_{\mathsf{i}} F_{\theta}(z) D_{\theta} \left(\eta_{\mathsf{a}}(z) - \hat{\eta}(z), \Delta \nu(z) \right) \tag{PLL}$$





Someshwar C Gupta, "Phase-Locked loops", In: Proc. IEEE 63.2 (1975), pp. 291–306

Dynamic and stochastic response (2/5)

Induced-Jamming and Induced-Spoofing Results

Linear Assumption:

LINEAR ASSUMPTION



¹ John W Betz and Kevin R Kolodziejski. "Generalized theory of code tracking with an early-late discriminator part II: Noncoherent processing and numerical results". In: IEEE Transactions on Aerospace and Electronic Systems 45.4 (2009), pp. 1557–1564.

Dynamic and stochastic response (2/5)

Induced-Jamming and Induced-Spoofing Results

Linear Assumption:

✓ The dynamic response can be analyzed through the **transfer function** of the equivalent linear closed-loop model $H_{\phi}(z)$:

$$\hat{\phi}^{(\mathsf{J})}(z) = H_{\phi}(z)\,\phi_{\mathsf{a}}, \qquad \hat{\phi}^{(\mathsf{S})}(z) = H_{\phi}(z)\,\phi_{\mathsf{s}}.$$

LINEAR ASSUMPTION



¹ John W Betz and Kevin R Kolodziejski. "Generalized theory of code tracking with an early-late discriminator part II: Noncoherent processing and numerical results." In: IEEE Transactions on Aerospace and Electronic Systems 45.4 (2009), pp. 1557–1564.

Emile Ghizzo - ENAC

Dynamic and stochastic response (2/5)

Induced-Jamming and Induced-Spoofing Results

Linear Assumption:

✓ The dynamic response can be analyzed through the **transfer function** of the equivalent linear closed-loop model $H_{\phi}(z)$:

$$\hat{\phi}^{(\mathsf{J})}(z) = H_{\phi}(z)\,\phi_{\mathsf{a}}, \qquad \hat{\phi}^{(\mathsf{S})}(z) = H_{\phi}(z)\,\phi_{\mathsf{s}}.$$

√ The noise is considered additive and homogeneous and can be modeled as presented for the nominal situation in the literature¹.

LINEAR ASSUMPTION



¹ John W Betz and Kevin R Kolodziejski. "Generalized theory of code tracking with an early-late discriminator part II: Noncoherent processing and numerical results". In: IEEE Transactions on Aerospace and Electronic Systems 45.4 (2009), pp. 1557–1564.

Dynamic and stochastic response (3/5)

Resolution Under Induced-Multipath Situation

Non-linear:

The system cannot be modeled using a transfer function.

$$\begin{cases} \hat{\tau}(z) + \beta \ \hat{\theta}(z) = \frac{z^{-1}}{1 - z^{-1}} T_{i} F_{\tau}(z) D_{\tau} \Big(\eta_{a}(z) - \hat{\eta}(z) , \Delta \nu(z) \Big) \\ \hat{\theta}(z) = \frac{z^{-1}}{1 - z^{-1}} T_{i} F_{\theta}(z) D_{\theta} \Big(\eta_{a}(z) - \hat{\eta}(z) , \Delta \nu(z) \Big) \end{cases}$$
(DLL)

$$\hat{\theta}(z) = \frac{z^{-1}}{1 - z^{-1}} T_{i} F_{\theta}(z) D_{\theta} \left(\eta_{a}(z) - \hat{\eta}(z), \Delta \nu(z) \right)$$
(PLL)







Dynamic and stochastic response (3/5)

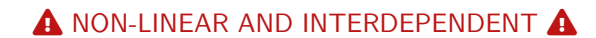
Resolution Under Induced-Multipath Situation

Non-linear:

The system cannot be modeled using a transfer function.

Random state vector
$$\hat{\phi}$$
 (ρ_{ϕ})

$$\begin{cases}
\hat{\tau}(z) + \beta \hat{\theta}(z) = \frac{z^{-1}}{1 - z^{-1}} T_{i} F_{\tau}(z) D_{\tau} \left(\eta_{a}(z) - \hat{\eta}(z), \Delta \nu(z) \right) \\
\hat{\theta}(z) = \frac{z^{-1}}{1 - z^{-1}} T_{i} F_{\theta}(z) D_{\theta} \left(\eta_{a}(z) - \hat{\eta}(z), \Delta \nu(z) \right)
\end{cases}$$
(PLL)







Dynamic and stochastic response (3/5)

Resolution Under Induced-Multipath Situation

Non-linear:

- × The system cannot be modeled using a transfer function.
- **Non-additivity:** Input dynamics and noise response cannot be separated.

Random state vector
$$\hat{\phi}(\rho_{\phi})$$

$$\begin{cases}
\hat{\tau}(z) + \beta & \hat{\theta}(z) = \frac{z^{-1}}{1 - z^{-1}} T_{i} F_{\tau}(z) D_{\tau} \left(\eta_{a}(z) - \hat{\eta}(z), \Delta \nu(z) \right) \\
\hat{\theta}(z) &= \frac{z^{-1}}{1 - z^{-1}} T_{i} F_{\theta}(z) D_{\theta} \left(\eta_{a}(z) - \hat{\eta}(z), \Delta \nu(z) \right)
\end{cases} (DLL)$$







Dynamic and stochastic response (3/5)

Resolution Under Induced-Multipath Situation

Non-linear:

- The system cannot be modeled using a transfer function.
- **Non-additivity:** Input dynamics and noise response cannot be separated.
- **Heterogeneity:** Noise variance depends on the system's actual state.

Random state vector
$$\hat{\phi}$$
 (p_{ϕ})

$$\begin{cases}
\hat{\tau}(z) + \beta & \hat{\theta}(z) = \frac{z^{-1}}{1 - z^{-1}} T_{i} F_{\tau}(z) D_{\tau} \left(\eta_{a}(z) - \hat{\eta}(z), \Delta \nu(z) \right) \\
\hat{\theta}(z) = \frac{z^{-1}}{1 - z^{-1}} T_{i} F_{\theta}(z) D_{\theta} \left(\eta_{a}(z) - \hat{\eta}(z), \Delta \nu(z) \right)
\end{cases}$$
(DLL)



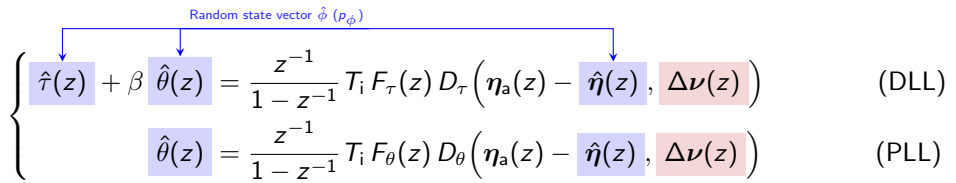




Dynamic and stochastic response (3/5)

Resolution Strategy

Quasi-Harmonic Behavior:



$$\hat{\theta}(z) = \frac{z^{-1}}{1 - z^{-1}} T_{i} F_{\theta}(z) D_{\theta} \left(\eta_{a}(z) - \hat{\eta}(z), \frac{\Delta \nu(z)}{2} \right)$$
(PLL)







Dynamic and stochastic response (3/5)

Resolution Strategy

Quasi-Harmonic Behavior:

• The system's SE exhibit oscillations along the relative phase $\Delta \theta$.

Random state vector
$$\hat{\phi}$$
 (ρ_{ϕ})

$$\begin{cases}
\hat{\tau}(z) + \beta \hat{\theta}(z) = \frac{z^{-1}}{1 - z^{-1}} T_{i} F_{\tau}(z) D_{\tau} \left(\eta_{a}(z) - \hat{\eta}(z), \Delta \nu(z) \right) \\
\hat{\theta}(z) = \frac{z^{-1}}{1 - z^{-1}} T_{i} F_{\theta}(z) D_{\theta} \left(\eta_{a}(z) - \hat{\eta}(z), \Delta \nu(z) \right)
\end{cases}$$
(PLL)







Dynamic and stochastic response (3/5)

Resolution Strategy

Quasi-Harmonic Behavior:

- The system's SE exhibit oscillations along the relative phase $\Delta \theta$.
- Other relative parameters, $\Delta \nu$, can be assumed constant over $\Delta \theta \in [0, 2\pi]$.

Random state vector
$$\hat{\phi}$$
 (ρ_{ϕ})

$$\begin{cases}
\hat{\tau}(z) + \beta \hat{\theta}(z) = \frac{z^{-1}}{1 - z^{-1}} T_{i} F_{\tau}(z) D_{\tau} \left(\eta_{a}(z) - \hat{\eta}(z), \Delta \nu(z) \right) \\
\hat{\theta}(z) = \frac{z^{-1}}{1 - z^{-1}} T_{i} F_{\theta}(z) D_{\theta} \left(\eta_{a}(z) - \hat{\eta}(z), \Delta \nu(z) \right)
\end{cases}$$
(DLL)







Dynamic and stochastic response (3/5)

Resolution Strategy

Quasi-Harmonic Behavior:

- The system's SE exhibit oscillations along the relative phase $\Delta \theta$.
- Other relative parameters, $\Delta \nu$, can be assumed constant over $\Delta \theta \in [0, 2\pi]$.
- The system behavior can be characterized by its quasi-harmonic response for any $\Delta \nu$.

$$\begin{cases}
\hat{\tau}(z) + \beta \quad \hat{\theta}(z) = \frac{z^{-1}}{1 - z^{-1}} T_{i} F_{\tau}(z) D_{\tau} \left(\eta_{a}(z) - \hat{\eta}(z), \Delta \nu \right) \\
\hat{\theta}(z) = \frac{z^{-1}}{1 - z^{-1}} T_{i} F_{\theta}(z) D_{\theta} \left(\eta_{a}(z) - \hat{\eta}(z), \Delta \nu \right)
\end{cases} \quad (DLL)$$







Dynamic and stochastic response (4/5)

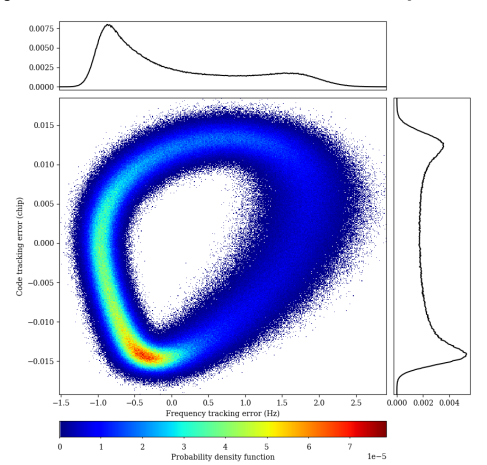
Induced-Multipath Results

Quasi-harmonic behavior:





Dynamic and stochastic response (4/5)



Tracking error PDF p_{ϕ} ($\Delta \tau = 0.5 \mathrm{chip}$, $\Delta f = 2 \mathrm{Hz}$, $\Delta g = 0.64 \mathrm{and} \ C/N_0 = 50 \mathrm{dB.Hz}$).

Induced-Multipath Results

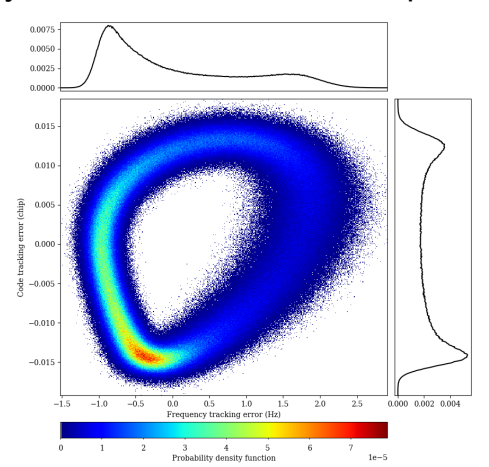
Quasi-harmonic behavior:

 \checkmark Enable the characterization of the tracking error under induced multipath as a function of the relative dynamics $\Delta \nu$ and receiver parameters.





Dynamic and stochastic response (4/5)



Tracking error PDF p_{ϕ} ($\Delta \tau = 0.5 \mathrm{chip}$, $\Delta f = 2 \mathrm{Hz}$, $\Delta g = 0.64 \mathrm{and} \ C/N_0 = 50 \mathrm{dB.Hz}$).

Induced-Multipath Results

Quasi-harmonic behavior:

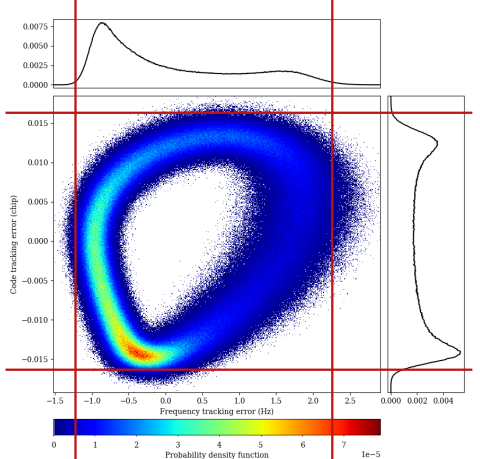
- \checkmark Enable the characterization of the tracking error under induced multipath as a function of the relative dynamics $\Delta \nu$ and receiver parameters.
- √ Accounts for the system's non-linearity, filtering, and stochastic aspects.





Post-correlator

Dynamic and stochastic response (4/5)



Tracking error PDF p_{ϕ} ($\Delta \tau = 0.5 \text{ chip}$, $\Delta f = 2$ Hz, $\Delta g = 0.64$ and $C/N_0 = 50$ dB.Hz).

Induced-Multipath Results

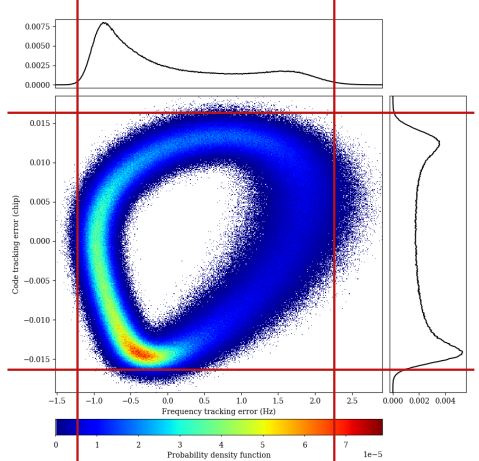
Quasi-harmonic behavior:

- ✓ Enable the characterization of the tracking error under induced multipath as a function of the relative dynamics $\Delta \nu$ and receiver parameters.
- Accounts for the **system's non-linearity**, filtering, and stochastic aspects.
- √ Enables the derivation of a more accurate. Spoofing Error Envelope (SEE).





Dynamic and stochastic response (4/5)



Tracking error PDF p_{ϕ} ($\Delta \tau = 0.5 \mathrm{chip}$, $\Delta f = 2 \mathrm{Hz}$, $\Delta g = 0.64 \mathrm{and} \ C/N_0 = 50 \mathrm{dB.Hz}$).

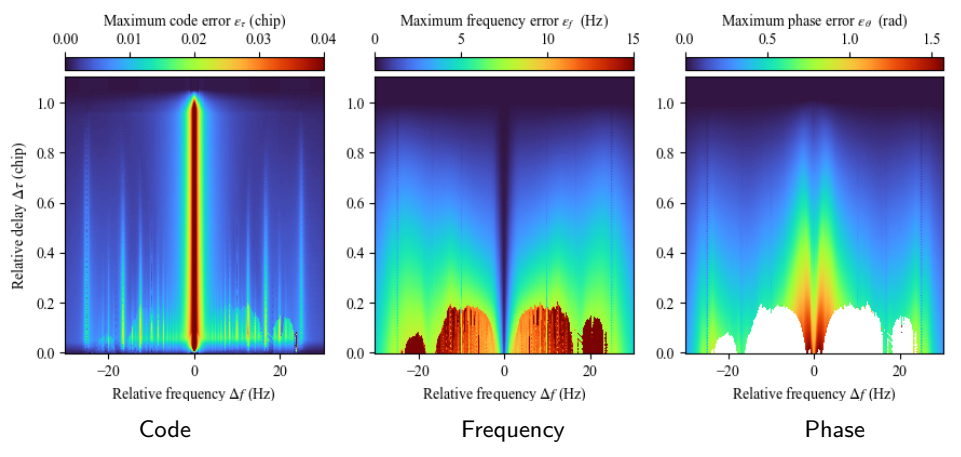
Induced-Multipath Results

Quasi-harmonic behavior:

- \checkmark Enable the characterization of the tracking error under induced multipath as a function of the relative dynamics $\Delta \nu$ and receiver parameters.
- ✓ Accounts for the system's non-linearity, filtering, and stochastic aspects.
- √ Enables the derivation of a more accurate
 Spoofing Error Envelope (SEE).
- X Does not model bifurcation or transient response.



Dynamic and stochastic response (5/5)



Absolute Spoofing Error Envelope ($\Delta g=0.64$ and authentic C/N_0 of 55 dB.Hz).





Outline

- Context
- 2 Received signal model under spoofing
- 3 Impact of spoofing before correlation
- 4 Impact of spoofing after correlation

 Correlator output

 Tracking loops

 C/N₀
- **5** Experimentation
- 6 Conclusion





C/N_0 definition

Objective

Characterize the true and estimated C/N_0 under each induced-spoofing situation.





C/N_0 definition

Objective

Characterize the true and estimated C/N_0 under each induced-spoofing situation.

True C/N_0 (over $\Omega \times I_t$):

$$\left(\frac{C}{N_0}\right)_{\text{true}} \triangleq \frac{1}{T_i} \frac{P_d}{P_s}$$





C/N_0 definition

Objective

Characterize the true and estimated C/N_0 under each induced-spoofing situation.

True
$$C/N_0$$
 (over $\Omega \times I_t$):

Useful signal power





Useful signal power

C/N_0 definition

Objective

Characterize the true and estimated C/N_0 under each induced-spoofing situation.

Post-correlator

True
$$C/N_0$$
 (over $\Omega \times I_t$):

$$\left(\frac{C}{N_0}\right)_{\text{true}} \triangleq \frac{1}{T_i} | \frac{P_d}{P_c} |$$
Normalization factor \uparrow Random signal power

Estimated C/N_0 (measured on the prompt correlator outputs over I_t): Three algorithms:

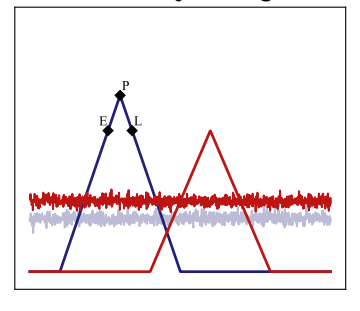
- Moment Method (MM) (equivalent to Variance Summing Method (VSM).
- Narrow Wideband Power Ratio (NWPR),
- Beaulieu method



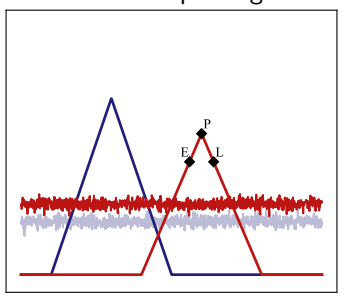


C/N_0 under spoofing (1/4)

Induced-jamming



Induced-spoofing





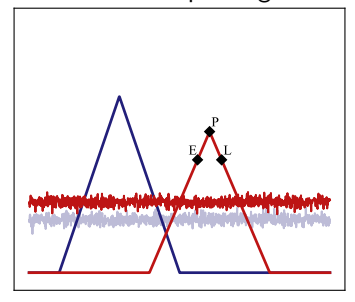


Induced-jamming

True C/N_0 :

$$\left(\frac{C}{N_0}\right)_{\text{true}}^{(J)} = \frac{1}{T_i} \frac{P_d}{P_\varsigma} = \frac{\zeta(\varepsilon_\eta)^2}{T_i} \frac{C_a}{P_n + P_\chi}$$

Induced-spoofing







Induced-jamming

Induced-spoofing

True C/N_0 :

$$\left(\frac{C}{N_0}\right)_{\rm true}^{\rm (J)} = \frac{1}{T_{\rm i}} \frac{P_{\rm d}}{P_{\varsigma}} = \frac{\zeta(\varepsilon_{\eta})^2}{T_{\rm i}} \frac{C_{\rm a}}{P_{n} + P_{\chi}}$$

True C/N_0 :

$$\left(\frac{C}{N_0}\right)_{\rm true}^{\rm (S)} = \frac{1}{T_{\rm i}} \frac{P_{\rm d}}{P_{\varsigma}} = \frac{\zeta(\varepsilon_{\eta} + \Delta \eta)^2}{T_{\rm i}} \frac{\Delta g \ C_{\rm a}}{P_{n} + P_{\chi}}$$

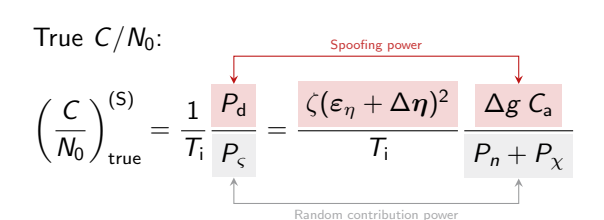




Induced-jamming

True C/N_0 :

Induced-spoofing



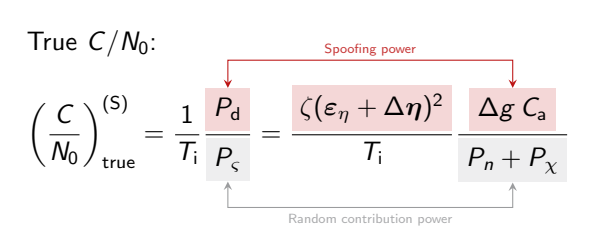




Induced-jamming

True C/N_0 : $\left(\frac{C}{N_0}\right)_{\text{true}}^{\text{(J)}} = \frac{1}{T_i} \frac{P_{\text{d}}}{P_{\varsigma}} = \frac{\zeta(\varepsilon_{\eta})^2}{T_i} \frac{C_{\text{a}}}{P_n + P_{\chi}}$ Random contribution power

Induced-spoofing



Induced-Jamming and Induced-Spoofing Results

The estimators are unbiased and converge to the true C/N_0 value.





Induced-multipath:





C/N_0 under spoofing (2/4) Prompt correlator evolution:





C/N_0 under spoofing (2/4)

Prompt correlator evolution:

True C/N_0 :

$$\left(\frac{C}{N_0}\right)_{\text{true}}^{(\text{M})} = \frac{1}{T_i} \frac{P_d}{P_c} = \frac{1}{T_i} \frac{\left(\frac{\mu_d}{\mu_d} + \frac{\omega_d}{\omega_d}\right) C_a}{P_n + P_\chi}.$$





C/N_0 under spoofing (3/4)

Induced-Multipath Results





Induced-Multipath Results

Derivation of analytic expressions as a function of $\Delta \eta$.

MM:

Interaction random power variance $\mathbb{E}_{\Omega} \left[\frac{\widehat{C}}{N_0} \right]_{\text{MM}}^{(\text{MI})} \approx \frac{1}{T_i} \frac{\sqrt{P_d^2 - C_a^2 \sigma_d^2}}{P_c + P_d - \sqrt{P_d^2 - C_a^2 \sigma_d^2}}$ Beaulieu:

$$\mathbb{E}_{\Omega} \left[\frac{\widehat{C}}{N_0} \right]_{\mathsf{B}}^{(\mathsf{M})} = \left[\frac{P_{\varsigma} + \delta_{\mathsf{B}}}{P_{\mathsf{d}}} - \varepsilon_{\mathsf{B}} \right]_{\mathsf{Beaulieu Non-ergodic error}}^{-1}$$

NWPR:

$$\mathbb{E}_{\Omega} \left[\frac{\widehat{C}}{N_0} \right]_{\text{NWPR}}^{(M)} \approx \frac{1}{T_i} \frac{P_{\text{d}} + \sigma_{\text{WB}} - \varepsilon_{\text{PR}}}{P_{\varsigma} - \sigma_{\text{WB}} + \varepsilon_{\text{PR}}/L}$$
NW band error \(\tag{PR non-e} \)





Induced-Multipath Results

- Derivation of **analytic expressions** as a function of $\Delta \eta$.
- The MM, Beaulieu, and NWPR estimators are **biased** and do not reflect the true C/N_0 .

MM:

 $\mathbb{E}_{\Omega} \left[\frac{\widehat{C}}{N_0} \right]_{\mathsf{MM}}^{(\mathsf{M})} \approx \frac{1}{T_{\mathsf{i}}} \frac{\sqrt{{P_{\mathsf{d}}}^2 - {C_{\mathsf{a}}}^2 \, \sigma_{\mathsf{d}}^2}}{\sqrt{{P_{\mathsf{d}}}^2 - {C_{\mathsf{a}}}^2 \, \sigma_{\mathsf{d}}^2}}$

Beaulieu:

$$\mathbb{E}_{\Omega} \left[\frac{\widehat{C}}{N_0} \right]_{\mathrm{B}}^{\mathrm{(M)}} = \left[\frac{P_{\varsigma} + \delta_B}{P_{\mathrm{d}}} - \varepsilon_B \right]^{-1}$$
Beaulieu Non-ergodic error

NWPR:

$$\mathbb{E}_{\Omega} \left[\frac{\widehat{C}}{N_0} \right]_{\text{NWPR}}^{(M)} \approx \frac{1}{T_i} \frac{P_{\text{d}} + \sigma_{\text{WB}} - \varepsilon_{\text{PR}}}{P_{\varsigma} - \sigma_{\text{WB}} + \varepsilon_{\text{PR}}/L}$$
NW band error \(\daggered{\tau} \) \(\text{PR non-e} \)





Induced-Multipath Results

- Derivation of analytic expressions as a function of $\Delta \eta$.
- The MM, Beaulieu, and NWPR estimators are **biased** and do not reflect the true C/N_0 .

Post-correlator

Spoofing distortion varies depending on the type of estimator.

MM:

Interaction random power variance $\mathbb{E}_{\Omega} \left[\frac{\widehat{C}}{N_0} \right]_{MM}^{(M)} \approx \frac{1}{T_i} \frac{\sqrt{P_d^2 - C_a^2 \sigma_d^2}}{P_c + P_d - \sqrt{P_d^2 - C_a^2 \sigma_d^2}}$ Beaulieu:

$$\mathbb{E}_{\Omega} \left[\frac{\widehat{C}}{N_0} \right]_{\mathsf{B}}^{\mathsf{(M)}} = \left[\frac{P_{\varsigma} + \delta_{\mathsf{B}}}{P_{\mathsf{d}}} - \varepsilon_{\mathsf{B}} \right]_{\mathsf{Beaulieu Non-ergodic error}}^{\mathsf{Correlator difference power}}$$

NWPR:

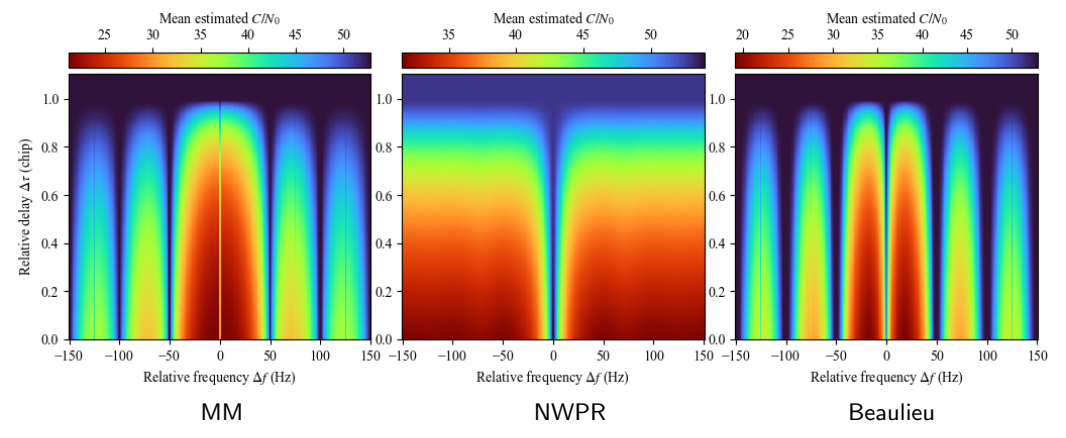
$$\mathbb{E}_{\Omega} \left[\frac{\widehat{C}}{N_0} \right]_{\text{NWPR}}^{(M)} \approx \frac{1}{T_i} \frac{P_{\text{d}} + \sigma_{\text{WB}} - \varepsilon_{\text{PR}}}{P_{\varsigma} - \sigma_{\text{WB}} + \varepsilon_{\text{PR}}/L}$$
NW band error \(\dagger) \quad \text{PR non-e}





Post-correlator

C/N_0 under spoofing (4/4)



Mean estimated C/N_0 in dB.Hz ($\Delta g = 0.64$ and authentic C/N_0 of 55 dB.Hz).





Conclusion

Spoofing Impact After Correlation

The impact of spoofing on post-correlation stages can be classified into four situations:

- **Nominal:** The reference scenario with no spoofing impact.
- Induced-Jamming: The receiver tracks the authentic dynamics, and the spoofing impact is reduced to re-radiated noise.
- Induced-Spoofing: The receiver tracks the spoofing dynamics and adapts to the characteristics of the spoofing signal.
- Induced-Multipath: The receiver tracks a composite of both signals:
 - ⚠ The tracking loops exhibit **chaotic behavior**, including multiple SE and non-linear effects, inducing varying tracking errors and possible bifurcations.
 - \triangle The C/N_0 estimators suffer significant degradation, potentially leading to loss-of-lock.





Outline

- Context
- 2 Received signal model under spoofing
- 3 Impact of spoofing before correlation
- 4 Impact of spoofing after correlation
- **5** Experimentation
- 6 Conclusion





ontext Received signal Pre-correlator Post-correlator Experimentation Conclusion

Experiment presentation

Objectives





Experiment presentation

Objectives

• Observe the distortions predicted by the theoretical model in a **realistic spoofing environment** using **real GNSS receivers**.





Experimentation 0000000000

Experiment presentation

Objectives

Observe the distortions predicted by the theoretical model in a realistic spoofing environment using real GNSS receivers.







Experimentation 0000000000

Experiment presentation

Objectives

Observe the distortions predicted by the theoretical model in a realistic spoofing environment using real GNSS receivers.







Experiment presentation

Objectives

• Observe the distortions predicted by the theoretical model in a **realistic spoofing environment** using **real GNSS receivers**.







Experimentation 0000000000

Experiment presentation

Objectives

- Observe the distortions predicted by the theoretical model in a realistic spoofing environment using real GNSS receivers.
- Evaluate the theoretical predictions against experimental results and compare different receiver architectures.







Experimentation

Experiment presentation

Objectives

- Observe the distortions predicted by the theoretical model in a realistic spoofing environment using real GNSS receivers.
- Evaluate the theoretical predictions against experimental results and compare different receiver architectures.



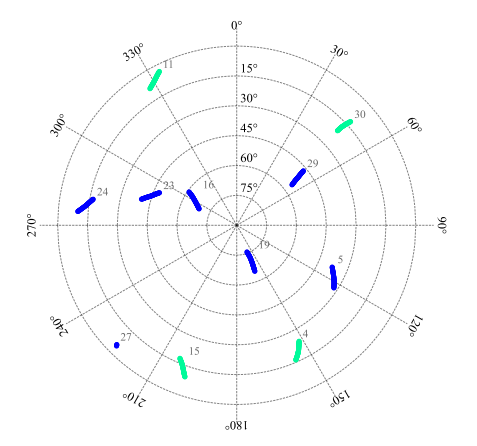
Examined Observables:

- Theoretical Models
- **Simulator:** Implements correlator, C/N_0 estimator, and tracking loops.
- Real Receivers:
 - GNSS SDR
 - Ifen SX3





Experiment scenario (1/2)

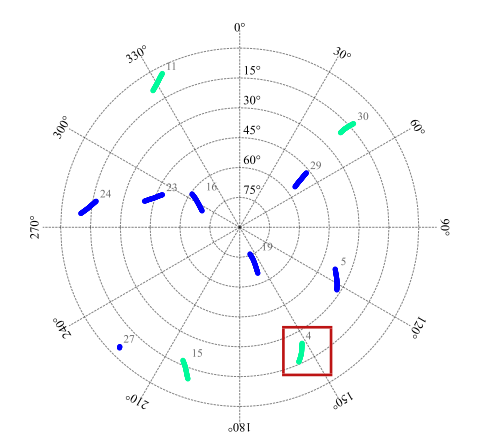






Experiment scenario (1/2)

PRN 4 analyzed (PRN 11, 15 and 30 in the manuscript)







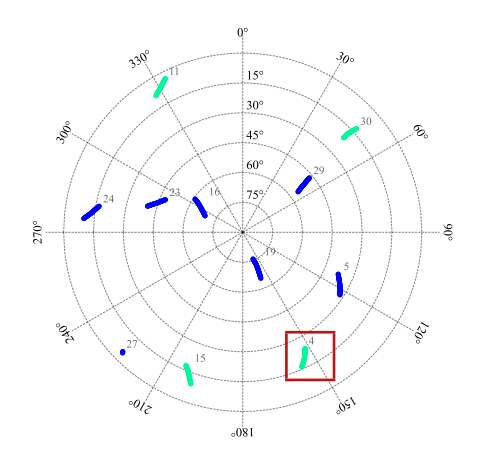
d signal Pre-correlator Post-correlator Experimentation

Experiment scenario (1/2)

PRN 4 analyzed (PRN 11, 15 and 30 in the manuscript)

Experiment Scenarios:

- Scenario 1: Nominal scenario (no spoofing).
- Scenario 2: Low-power sophisticated repeater without re-radiated noise.
- Scenario 3: High-power sophisticated repeater without re-radiated noise.







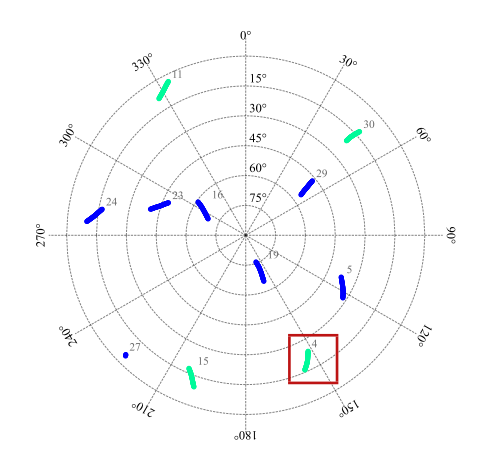
Experiment scenario (1/2)

PRN 4 analyzed (PRN 11, 15 and 30 in the manuscript)

Experiment Scenarios:

- Scenario 1: Nominal scenario (no spoofing).
- Scenario 2: Low-power sophisticated repeater without re-radiated noise.
- Scenario 3: High-power sophisticated repeater without re-radiated noise.

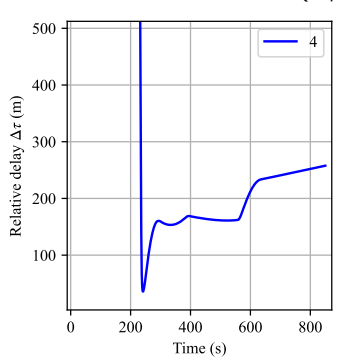
Same authentic dynamics: $\tau_{\rm a}(t)$, $\theta_{\rm a}(t)$, and same spoofing dynamics: $\tau_{\rm s}(t)$, $\theta_{\rm s}(t)$ across each scenario.

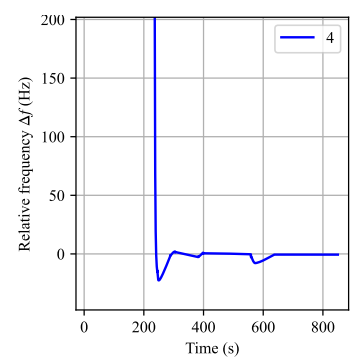


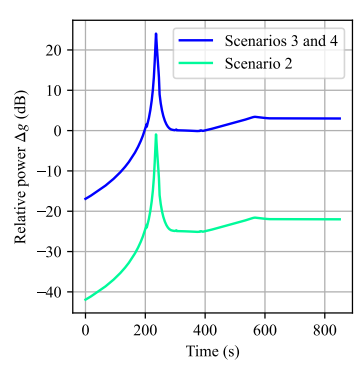




Experiment scenario (2/2)





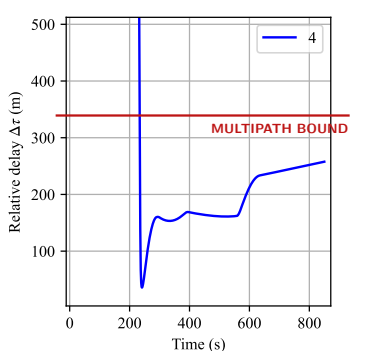


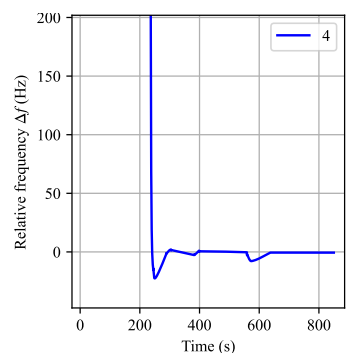
Relative parameters (code, frequency, power) for PRN 4.

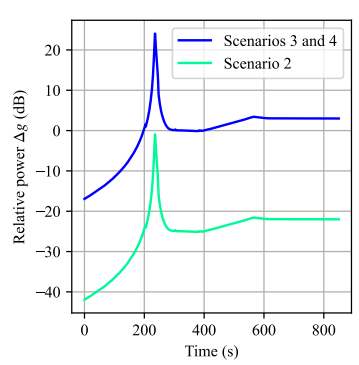




Experiment scenario (2/2)





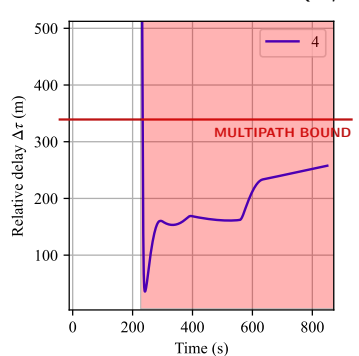


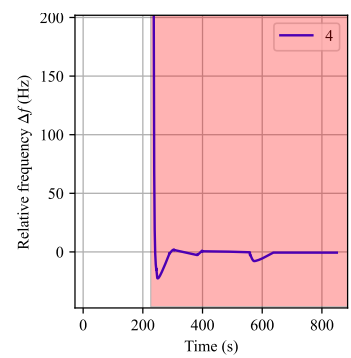
Relative parameters (code, frequency, power) for PRN 4.

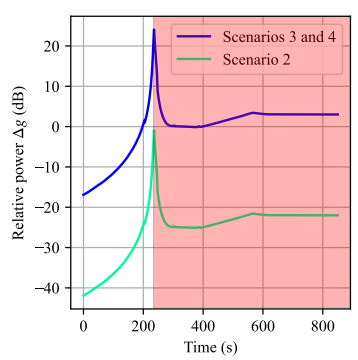




Experiment scenario (2/2)





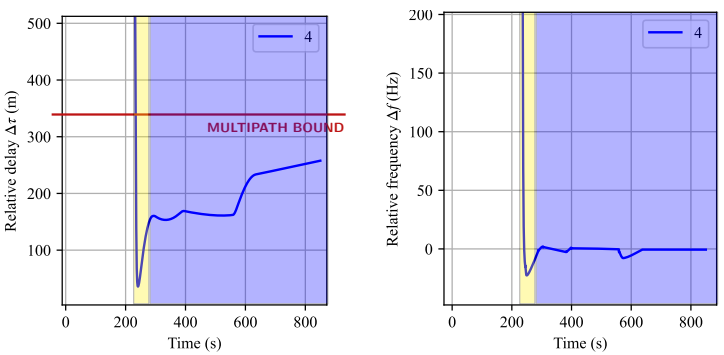


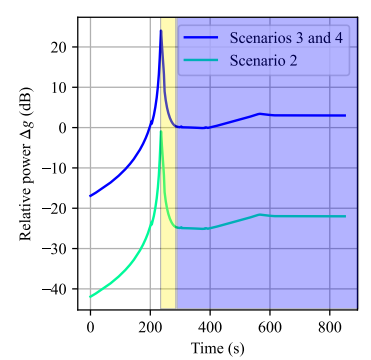
Relative parameters (code, frequency, power) for PRN 4.





Experiment scenario (2/2)





Relative parameters (code, frequency, power) for PRN 4.

: Flying over the spoofer / Landing (high dynamics)

: Taxiing (low dynamics)





Experiment setup

		SX3	GNSS-SDR	Simulator	
Acquisition		$Doppler = \pm 5000 \text{ Hz}$		$Doppler = \pm 3500 \text{ Hz}$	
		Coherent time = 1 ms, Incoherent number = 10, $P_{\text{Fa}} = 10^{-3}$			
Tracking correlator		Integration time $T_{\rm i}=10~{ m ms}$			
DLL	Discriminator	EMLP	EMLE	EMLP	
		$c_{ au} = 0.1 ext{ chip}$			
	Low-pass filter	1st order, $B_{\tau} = 1$ Hz			
	Loss indicator	Duration: 1 s, Type: C/N_0 , Threshold $\gamma_{\tau}=25~\mathrm{dB\cdot Hz}$			
PLL	Discriminator	Costas loop (unknown)	Costas loop (atan)		
	Low-pass filter	$B_{\theta} = 20 \text{ Hz}$	$B_{\theta} = 30 \text{ Hz}$	$B_{\theta} = 20 \text{ Hz}$	
		3rd order			
	Loss indicator	Not used	NECT, Duration: 1 s,	Not used	
			Threshold $\gamma_{\theta} = 0.85$		
C/N_0 estimation		Signal power/Noise power	Type: MM		
		Estimation period: 1 s			





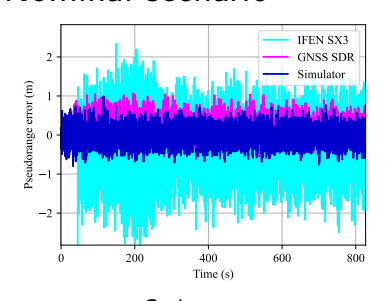
Experiment setup

		SX3	GNSS-SDR	Simulator	
Acquisition		$Doppler = \pm 5000 \text{ Hz}$		$Doppler = \pm 3500 \; Hz$	
		Coherent time = 1 ms, Incoherent number = 10, $P_{\text{Fa}} = 10^{-3}$			
Tracking correlator		Integration time $T_{\rm i}=10~{ m ms}$			
DLL	Discriminator	EMLP	EMLE	EMLP	
		$c_{ au} = 0.1 ext{ chip}$			
	Low-pass filter	1st order, $B_{\tau} = 1$ Hz			
	Loss indicator	Duration: 1 s, Type: C/N_0 , Threshold $\gamma_{\tau}=25~\mathrm{dB\cdot Hz}$			
PLL	Discriminator	Costas loop (unknown)	Costas loop (atan)		
	Low-pass filter	$B_{\theta} = 20 \; \mathrm{Hz}$	$B_{\theta} = 30 \text{ Hz}$	$B_{\theta} = 20 \text{ Hz}$	
		3rd order			
	Loss indicator	Not used	NECT, Duration: 1 s,	Not used	
			Threshold $\gamma_{\theta} = 0.85$		
C/N_0 estimation		Signal power/Noise power	Type: MM		
		Estimation period: 1 s			





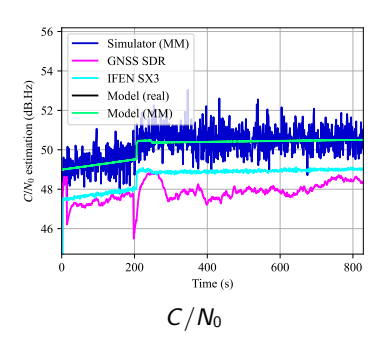
Nominal scenario



7.5 GNSS SDR Simulator
1.5 0.0 INFEN SX3

2.5 0.0 INFEN SX3

-7.5 0 INFEN SX3



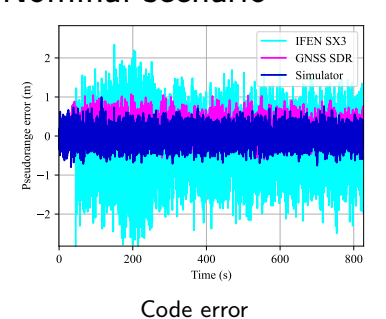
Code error

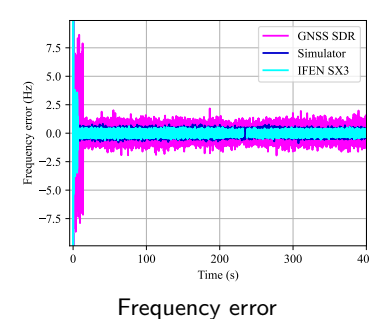
Frequency error

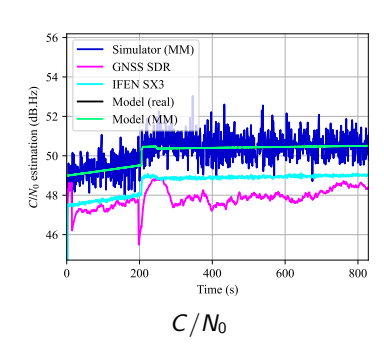




Nominal scenario





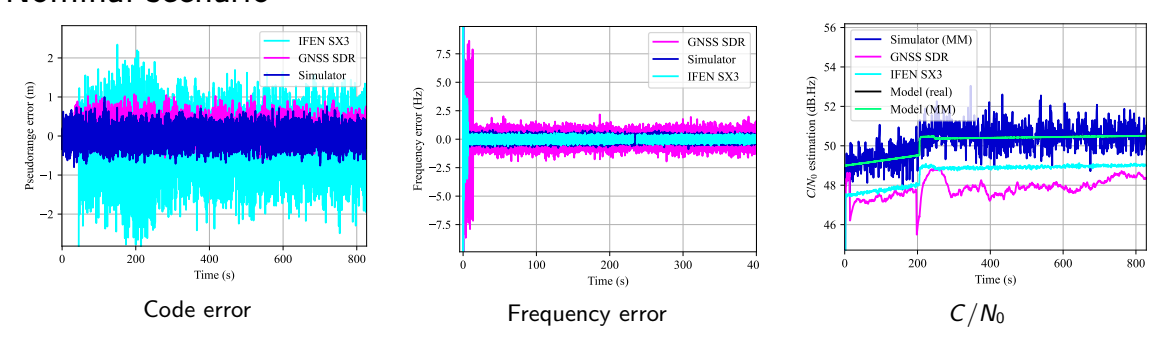


Experimental Errors:





Nominal scenario



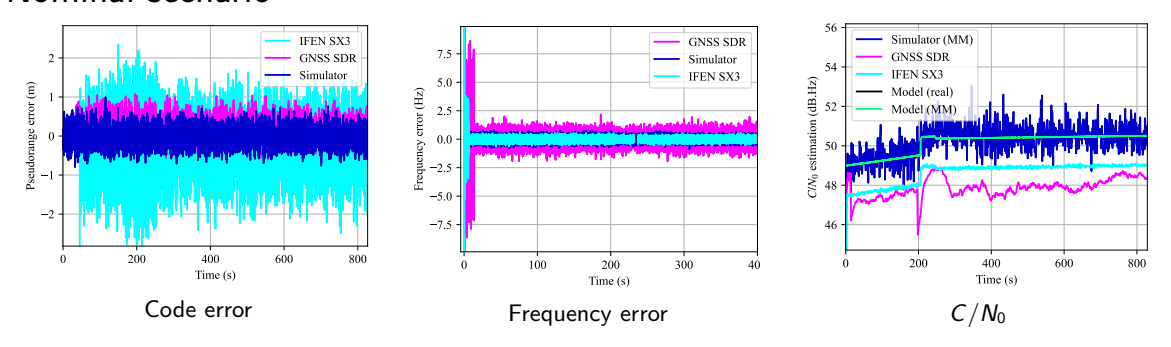
Experimental Errors:

• Additional noise in the SX3 code tracking error (possibly due to clock correction of the pseudorange).





Nominal scenario

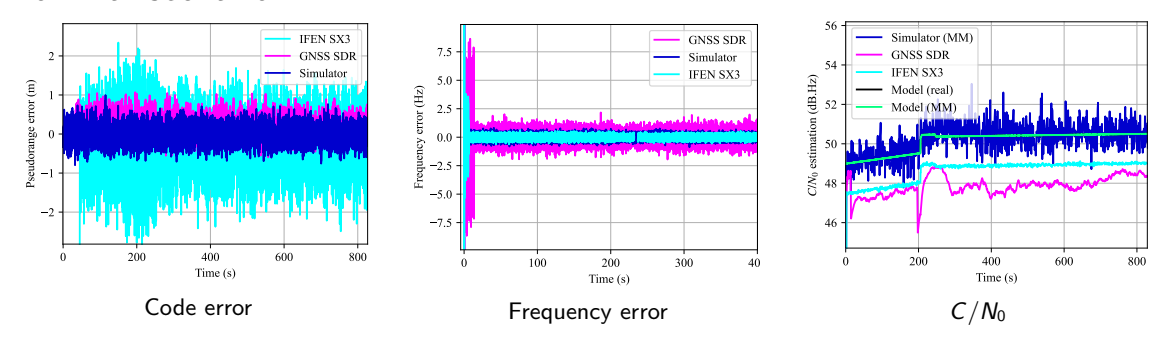


Experimental Errors:

- Additional noise in the SX3 code tracking error (possibly due to clock correction of the pseudorange).
- The SX3 and GNSS-SDR C/N_0 estimators **are biased** (constant bias but show the same trend as the expected C/N_0).



Nominal scenario

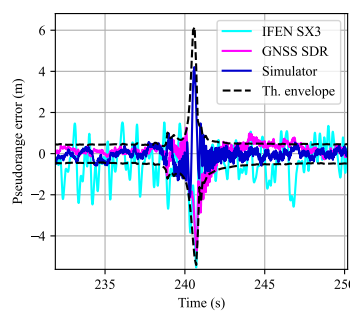


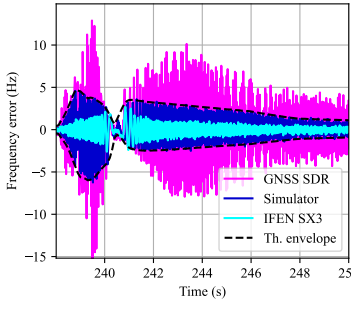
Experimental Errors:

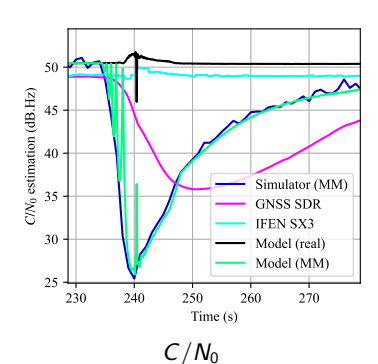
- Additional noise in the SX3 code tracking error (possibly due to clock correction of the pseudorange).
- The SX3 and GNSS-SDR C/N_0 estimators **are biased** (constant bias but show the same trend as the expected C/N_0).
- The GNSS-SDR C/N_0 estimators appear to be low-pass filtered.



Low-power repeater scenario - Landing phase







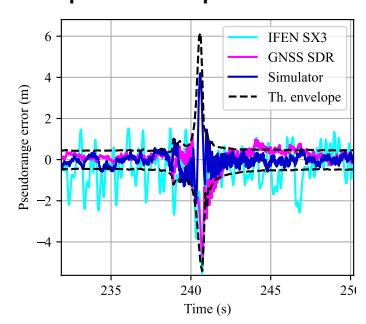
Code error

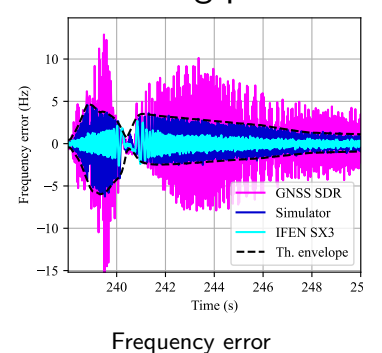
Frequency error

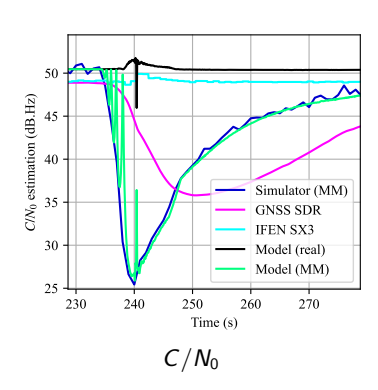




Low-power repeater scenario - Landing phase







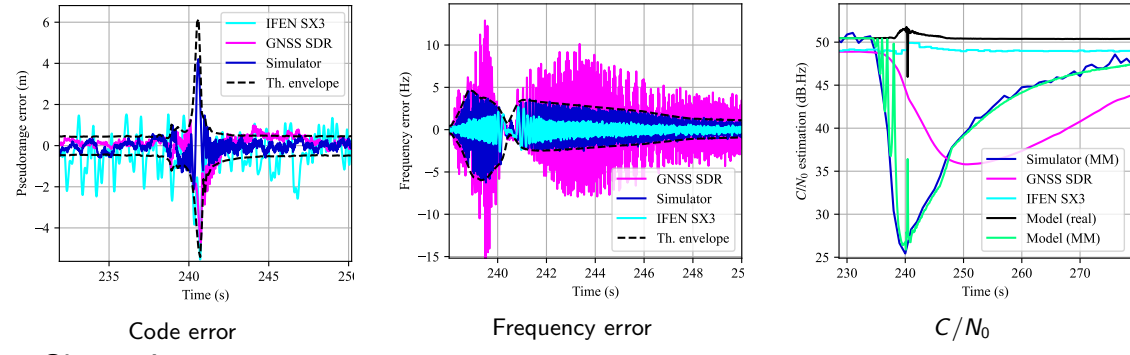
Code error

Observations:





Low-power repeater scenario - Landing phase



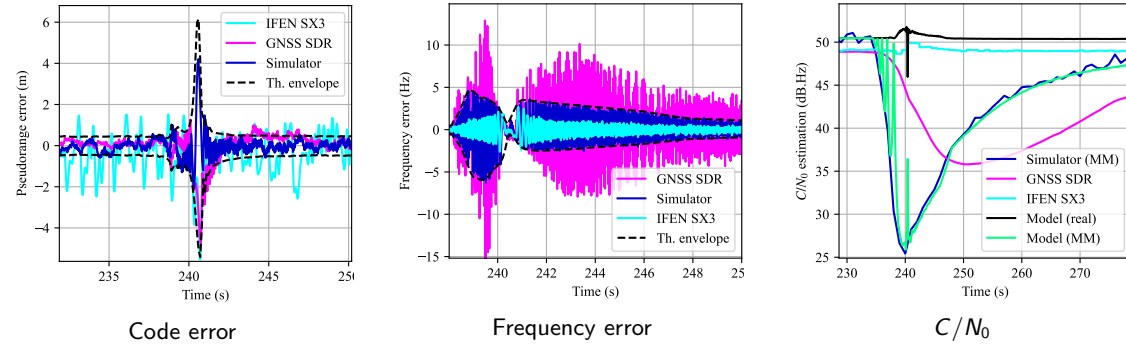
Observations:

• Tracking Errors: **oscillations** observed (dependence on the **receiver architecture**).





Low-power repeater scenario - Landing phase



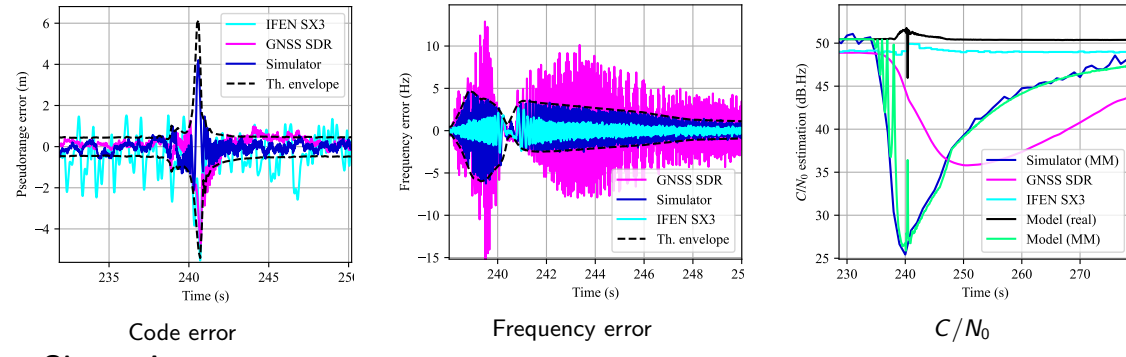
Observations:

- Tracking Errors: **oscillations** observed (dependence on the **receiver architecture**).
- C/N_0 Degradation: **Significant degradation** observed (strong **dependence** on the estimator method).





Low-power repeater scenario - Landing phase



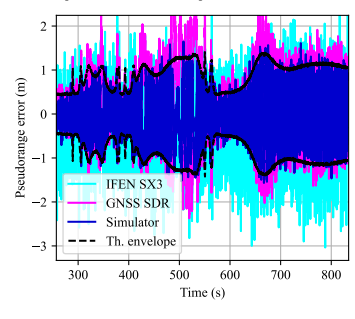
Observations:

- Tracking Errors: **oscillations** observed (dependence on the **receiver architecture**).
- C/N_0 Degradation: **Significant degradation** observed (strong **dependence** on the estimator method).
- The theoretical models accurately predict receiver behavior under spoofing conditions.

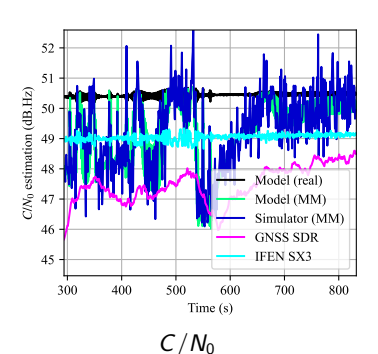




Low-power repeater scenario - Taxiing phase



GNSS SDR Simulator IFEN SX3 - Th. envelope - Th. envelope - The system of the system o



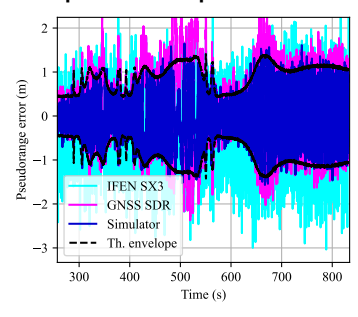
Code error

Frequency error





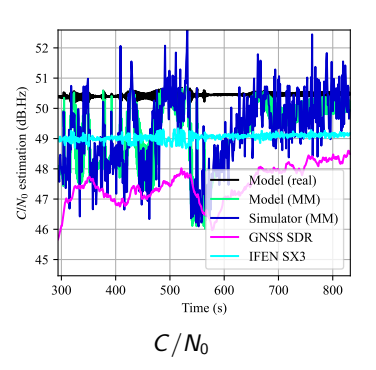
Low-power repeater scenario - Taxiing phase



GNSS SDR Simulator IIFEN SX3

The envelope of the property of

Frequency error



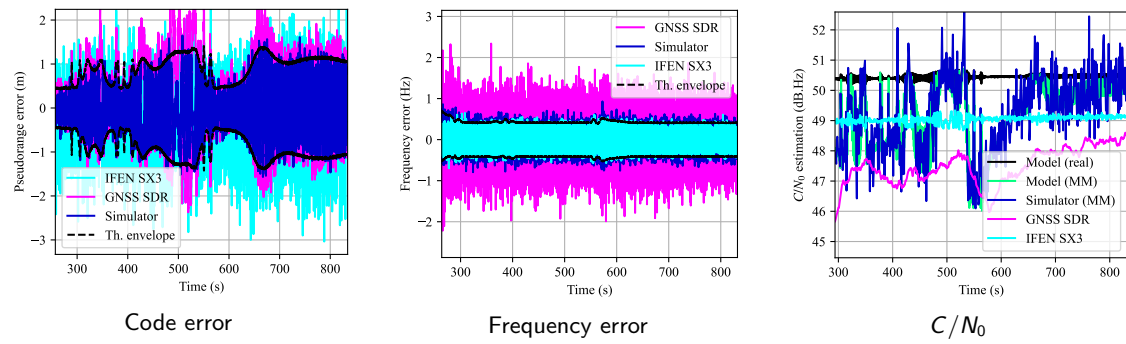
Code error

Observations:





Low-power repeater scenario - Taxiing phase



Observations:

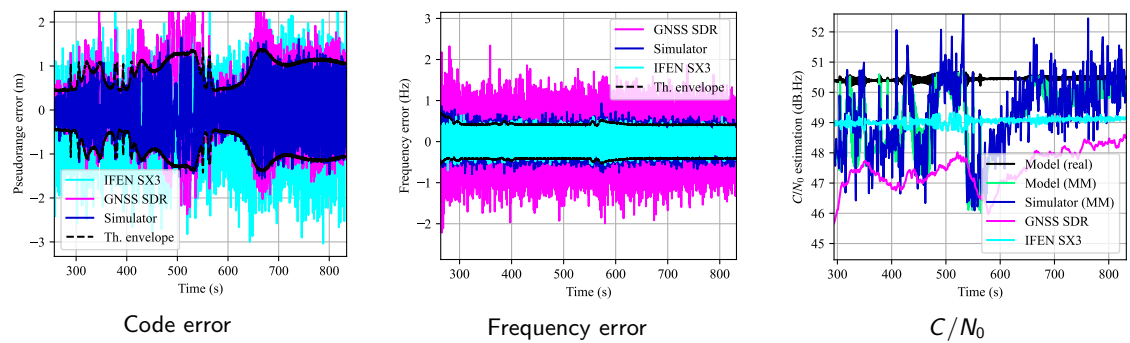
• Low oscillations in tracking errors and C/N_0 degradation ranging from 0.5 to 2 dB (dependence on the **receiver architecture**).





Experimentation obooppoop

Low-power repeater scenario - Taxiing phase



Observations:

- Low oscillations in tracking errors and C/N_0 degradation ranging from 0.5 to 2 dB (dependence on the receiver architecture).
- Observed distortion even at very low spoofing received power, $\Delta g < -20$ dB.

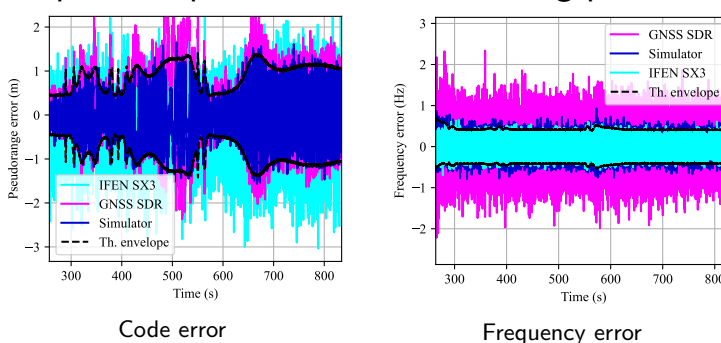


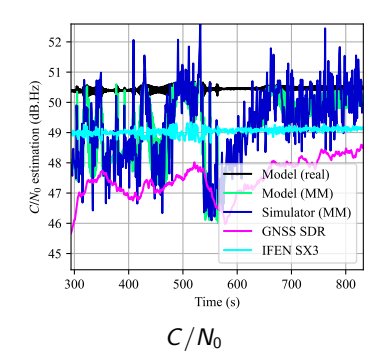


Experimentation

800

Low-power repeater scenario - Taxiing phase





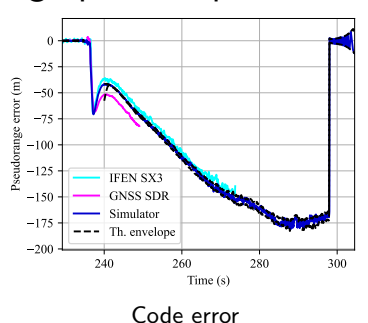
Observations:

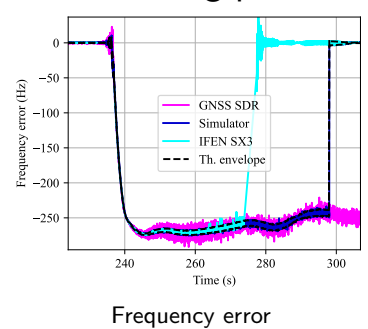
- Low oscillations in tracking errors and C/N_0 degradation ranging from 0.5 to 2 dB (dependence on the receiver architecture).
- Observed distortion even at very low spoofing received power, $\Delta g < -20$ dB.
- The theoretical models accurately predict receiver behavior under spoofing conditions.

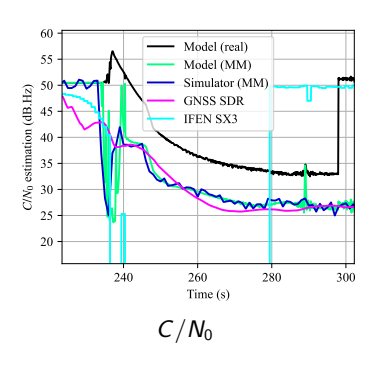




High-power repeater scenario - Landing phase





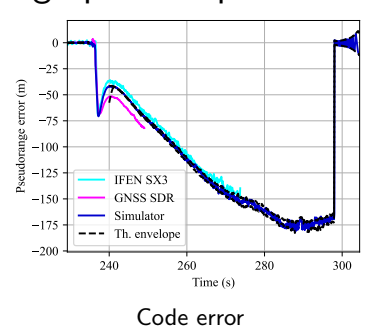


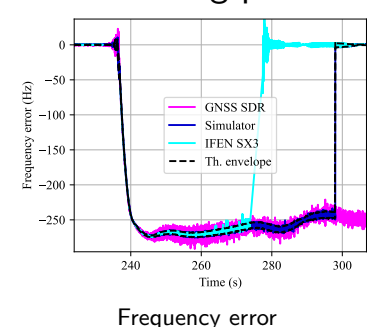
Observations:

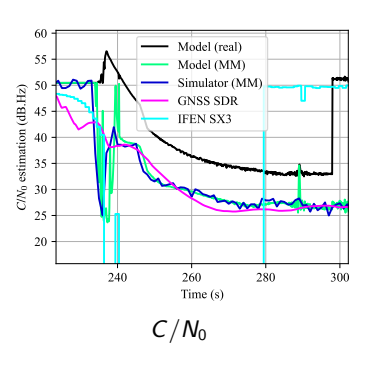




High-power repeater scenario - Landing phase







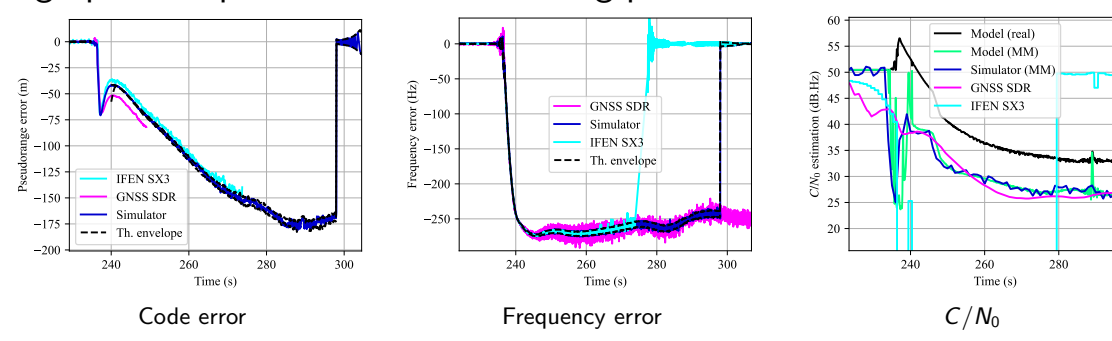
Observations:

• **Bifurcation** toward the 250 Hz-mismatched spoofing SE.





High-power repeater scenario - Landing phase



Observations:

- Bifurcation toward the 250 Hz-mismatched spoofing SE.
- Loss-of-lock as the received spoofing power decreases, followed by re-acquisition on the authentic SE.

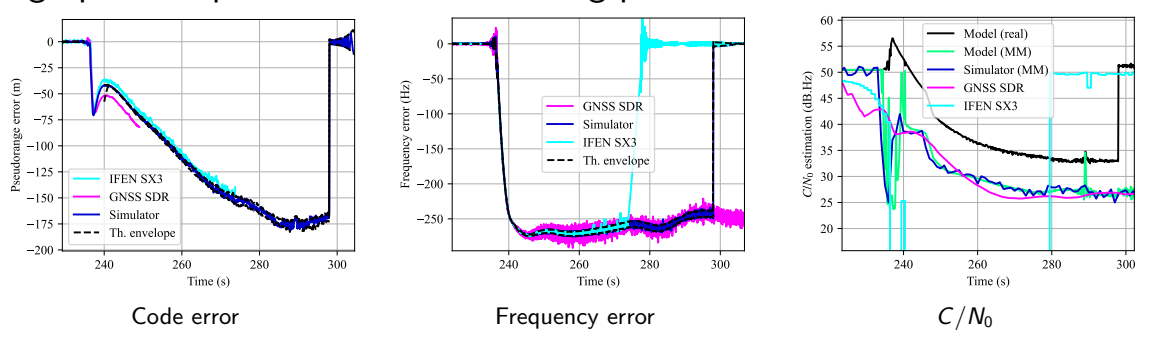




300

Experimentation

High-power repeater scenario - Landing phase



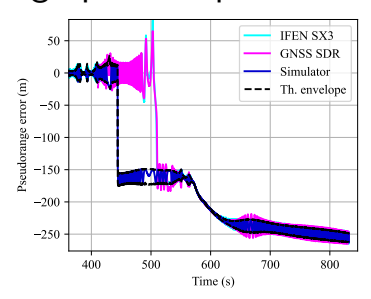
Observations:

- **Bifurcation** toward the 250 Hz-mismatched spoofing SE.
- Loss-of-lock as the received spoofing power decreases, followed by re-acquisition on the authentic SE.
- The model predicts the possible SE to which the system converges, as well as the FRANCAISE C/N_0 behavior.

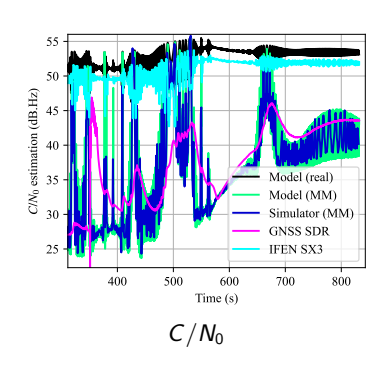




High-power repeater scenario - Taxiing phase



Frequency error



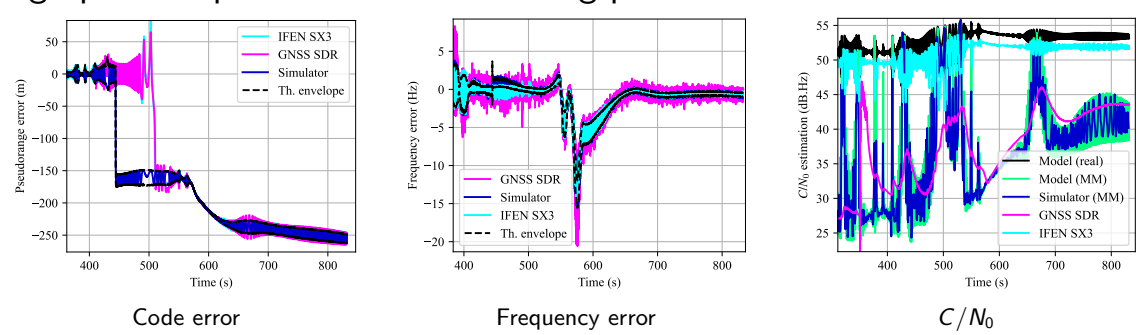
Code error

Observations:





High-power repeater scenario - Taxiing phase



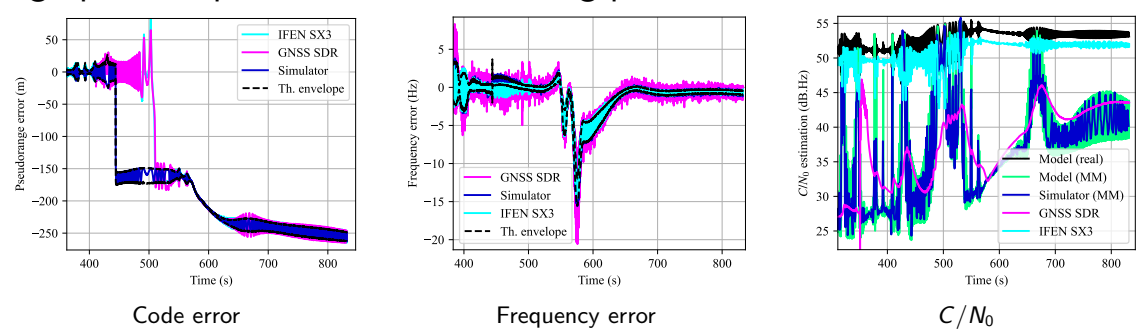
Observations:

• Tracking errors: **Strong oscillations** and **bifurcation** toward the spoofing SE (**chaotic behavior** with high dependence on the receiver architecture and environment).





High-power repeater scenario - Taxiing phase



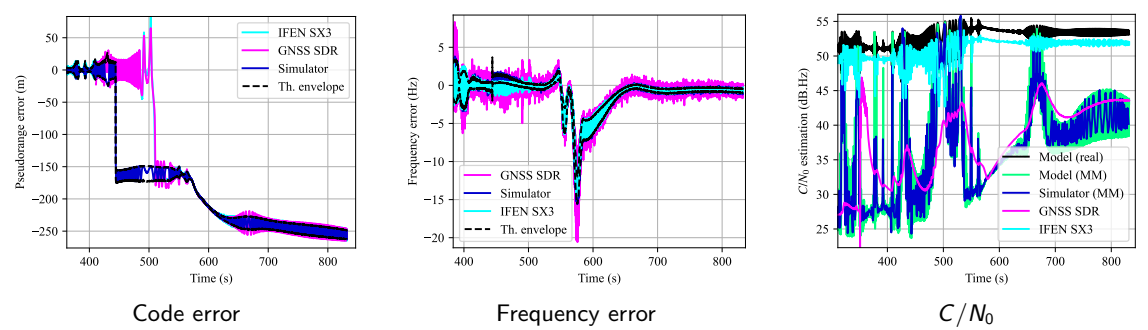
Observations:

- Tracking errors: **Strong oscillations** and **bifurcation** toward the spoofing SE (**chaotic behavior** with high dependence on the receiver architecture and environment).
- C/N_0 degradation: **Significant degradation** with method dependence and possible **loss-of-locks** (e.g., simulator at t = 450 s, followed by re-acquisition on the spoofing SE).



Experimentation

High-power repeater scenario - Taxiing phase



Observations:

- Tracking errors: Strong oscillations and bifurcation toward the spoofing SE (chaotic **behavior** with high dependence on the receiver architecture and environment).
- C/N_0 degradation: Significant degradation with method dependence and possible **loss-of-locks** (e.g., simulator at t = 450 s, followed by re-acquisition on the spoofing SE).
- The model accurately predicts the **possible SE** to which the system converges. as well as the C/N_0 behavior (and potential loss-of-locks).





Conclusion

```
Experiment observations
```





Experimentation 0000000000

Conclusion

Experiment observations



A The harmful distortion observed under induced-multipath situation, as exhibited in the theoretical models, is also observed in realistic spoofing environments.





Experimentation oooooooo

Conclusion

Experiment observations



A The harmful distortion observed under induced-multipath situation, as exhibited in the theoretical models, is also observed in realistic spoofing environments.



⚠ The experiments highlight the strong chaotic behavior of the GNSS receiver under such distortion, including tracking loop bifurcations, loss-of-lock, and a strong dependence on both the receiver architecture and the spoofing environment.





Conclusion

Experiment observations



A The harmful distortion observed under induced-multipath situation, as exhibited in the theoretical models, is also observed in realistic spoofing environments.



A The experiments highlight the strong chaotic behavior of the GNSS receiver under such distortion, including tracking loop bifurcations, loss-of-lock, and a strong dependence on both the receiver architecture and the spoofing environment.

However, the models proposed in this thesis provide accurate predictions of the possible loop SE and C/N_0 degradation, offering a means to understand and quantify the impact of spoofing.





Outline

- Context
- 2 Received signal model under spoofing
- 3 Impact of spoofing before correlation
- 4 Impact of spoofing after correlation
- **5** Experimentation
- **6** Conclusion





Conclusion 000

General Conclusions

Measure-Theory Framework

Introduction of a measure-theoretic framework for estimation under non-ergodic conditions:





General Conclusions

Measure-Theory Framework

Introduction of a measure-theoretic framework for estimation under non-ergodic conditions:

• Provide formal definitions for **signal power**, **independence**, **and expectation**.





Measure-Theory Framework

Introduction of a measure-theoretic framework for estimation under non-ergodic conditions:

- Provide formal definitions for **signal power**, **independence**, **and expectation**.
- Derive properties related to **stationarity** and **ergodicity**.





Measure-Theory Framework

Introduction of a measure-theoretic framework for estimation under non-ergodic conditions:

- Provide formal definitions for signal power, independence, and expectation.
- Derive properties related to **stationarity** and **ergodicity**.

Receiver Behavior Under Spoofing

Derivation of the theoretical model for the impact of spoofing before correlation (AGC, IF signal) and after correlation (Correlator outputs, tracking loops, and C/N_0):



Measure-Theory Framework

Introduction of a measure-theoretic framework for estimation under non-ergodic conditions:

- Provide formal definitions for signal power, independence, and expectation.
- Derive properties related to **stationarity** and **ergodicity**.

Receiver Behavior Under Spoofing

Derivation of the theoretical model for the impact of spoofing before correlation (AGC, IF signal) and after correlation (Correlator outputs, tracking loops, and C/N_0):

• **Pre-Correlation:** Spoofing acts as a multiple **weighted CW jammer** for the AGC, starting to impact AGC values when S/N > -5 dB.



Measure-Theory Framework

Introduction of a measure-theoretic framework for estimation under non-ergodic conditions:

- Provide formal definitions for signal power, independence, and expectation.
- Derive properties related to **stationarity** and **ergodicity**.

Receiver Behavior Under Spoofing

Derivation of the theoretical model for the impact of spoofing before correlation (AGC, IF signal) and after correlation (Correlator outputs, tracking loops, and C/N_0):

- **Pre-Correlation:** Spoofing acts as a multiple **weighted CW jammer** for the AGC, starting to impact AGC values when S/N > -5 dB.
- Post-Correlation: The impact of spoofing is categorized into four situations, including a harmful case where the receiver exhibits chaotic behavior, inducing **high tracking errors** and **significant** C/N_0 **degradation**, as well as, possible **tracking bifurcations** and **loss-of-locks**.



Thank You!

emile.ghizzo@alumni.enac.fr